

湘中地区龙山金锑矿床酸性岩脉 U-Pb 年代学和 Hf 同位素特征及其地质意义^{*}

陈佑纬 毕献武^{**} 付山岭 董少花

CHEN YouWei, BI XianWu^{**}, FU ShanLing and DONG ShaoHua

中国科学院地球化学研究所矿床地球化学国家重点实验室,贵阳 550081

State Key Laboratory of Ore Deposit Geochemistry, Institute of Geochemistry, Chinese Academy of Sciences, Guiyang 550081, China

2016-05-30 收稿, 2016-08-22 改回.

Chen YW, Bi XW, Fu SL and Dong SH. 2016. Zircon U-Pb dating and Hf isotope of the felsic dykes in the Longshan Au-Sb deposit in Central Hunan Province and their geological significance. *Acta Petrologica Sinica*, 32(11):3469–3488

Abstract This study presents a systematic geochemistry, zircon U-Pb dating and Hf isotope analysis on the felsic dykes outcropped around the Longshan Au-Sb deposit, aiming to constrain the intrusion ages, nature of sources and the tectonic setting of these felsic dykes and provide some new insights on the genetic relationship between the Longshan Au-Sb mineralization and magmatism. Zircon U-Pb dating results show that the felsic dykes occurred in five different locations around the Longshan Au-Sb deposit yield the same crystallization ages of 220~217 Ma (Late Indosinian). The Hf isotopes of the felsic dykes show the nearly identical characteristics with $^{176}\text{Hf}/^{177}\text{Hf}$ ratio of 0.282264~0.282536, $\varepsilon_{\text{Hf}}(t) = -13.4 \sim -3.7$, t_{DM2} of 2089~1482 Ma. Combining with the elements geochemical characteristics, it suggests that the felsic dykes may have derived from the partial melting of the Paleoproterozoic-Mesoproterozoic meta-sedimentary under a post-collision extensional tectonic setting. The intrusion ages of the felsic dykes are roughly consistent with the ore-forming age of the Longshan Au-Sb deposit, implying that deep-seated magmatism under the deposit may have supplied the part of mineralization hydrothermal fluid components and heat based on the previous studies.

Key words Longshan Au-Sb deposit; Felsic dykes; Zircon U-Pb age; Hf isotope; Central Hunan Province

摘要 本研究选择龙山金锑矿床外围出露的酸性岩脉(花岗斑岩脉、花岗闪长斑岩脉)开展系统的地球化学、锆石 U-Pb 年代学及 Hf 同位素研究, 以查明湘中盆地内酸性岩脉的形成时代、源区特征及构造背景, 并探讨了酸性岩脉与龙山金锑矿床的关系。锆石 U-Pb 定年结果显示, 龙山地区出露的 5 条酸性岩脉具有一致的结晶年龄, 为 220~217 Ma, 是印支晚期岩浆活动的产物。酸性岩脉的锆石 Lu-Hf 同位素组成特征也较为一致, $^{176}\text{Hf}/^{177}\text{Hf}$ 比值为 0.282264~0.282536, $\varepsilon_{\text{Hf}}(t) = -13.4 \sim -3.7$, t_{DM2} 为 2089~1482 Ma。结合元素地球化学特征, 表明龙山地区出露的酸性岩脉可能主要由深部的古-中元古代浅变质碎屑岩在碰撞后伸展背景下减压部分熔融形成。酸性岩脉的成岩年龄与龙山金锑矿印支晚期成矿年龄大体一致。结合前人的研究, 我们认为印支晚期的岩浆活动可能是龙山金锑矿成矿的重要热源和流体来源之一。

关键词 龙山金锑矿床; 酸性岩脉; 锆石 U-Pb 年龄; Hf 同位素; 湘中地区

中图法分类号 P597.3; P588.13

湘中地区(包括雪峰隆起东部)锑金矿带是中国西南大面积低温成矿域的重要组成部分(刘继顺, 1996; 马东升等, 2002; 涂光炽, 2002; 胡瑞忠等, 2007, 2015; Hu and Zhou, 2012)。其内分布着众多锑-金矿床, 如锡矿山超大型锑矿床、渣滓溪超大型锑矿床、沃溪大型钨金锑床、龙山大型锑金矿床等, 是我国重要的锑、金生产基地之一。

以往对该区的金锑矿床做了大量系统的研究工作, 如成矿地质特征、流体演化、物质来源、成矿时代和矿床成因等方面(罗献林, 1989; 刘继顺, 1993; 史明魁等, 1994; 毛景文和李红艳, 1997; 裴荣富等, 1998; 卢新卫, 1999; 彭渤和陈广浩, 2000; 鲍肖等, 2000; 彭建堂和胡瑞忠, 2001; 彭建堂等, 2002; 马东升等, 2002, 2003; Peng et al., 2003; Peng

* 本文受国家“973”项目(2014CB440902)和国家自然科学基金项目(41230316, 41473049, 41103027)联合资助。

第一作者简介: 陈佑纬, 男, 1983 年生, 博士, 副研究员, 从事矿床地球化学和岩石学研究, E-mail: chenyouwei@mail.gyig.ac.cn

** 通讯作者: 毕献武, 女, 1967 年生, 博士, 研究员, 从事矿床地球化学和岩石学研究, E-mail: bixianwu@vip.gyig.ac.cn

and Frei, 2004; 胡瑞忠等, 2007; 李华芹等, 2008; 陈新跃等, 2012; 刘升友等, 2013), 取得了许多重要的认识: 矿床产出主要受控于断裂带; 成矿流体具有大气降水和岩浆水等的混合特征; 成矿物质具有沉积地层、深部岩浆等多来源特征; 成矿时代主要为加里东期和印支-燕山期等。同时已有研究表明, 尽管金锑矿床产于基本无岩浆活动或岩浆活动很弱的沉积岩和浅变质岩系中(马东升等, 2002), 但一些锑金矿床与酸性岩脉呈现出较紧密的空间关系, 一些锑金矿脉赋存在岩脉内或其两侧的蚀变破碎带, 零星出露的长英质岩脉中常发生矿化(黄业明, 1996; 刘继顺, 1996; 鲍肖等, 2000)。根据酸性岩脉与 Au-Sb 矿化的紧密空间关系及部分酸性岩脉具有极高的锑金含量, 有学者建议可将其作为该区锑金矿的找矿标志(刘继顺, 1996; 鲍肖等, 2000; 彭渤和陈广浩, 2000; 鲍振襄等, 2002; 康如华, 2002; 孙际茂等, 2007)。但是, 以往对这些岩脉的研究主要集中于成矿元素含量测试及其与矿脉的空间关系描述上, 对酸性岩脉的精确年代学、地球化学、源区特征等的研究则很缺乏, 这极大地阻碍了对岩脉的成因及其与锑金成矿关系的深入认识。

龙山金锑矿是湘中地区金锑成矿带中典型的金锑共生矿床, 是湘中地区最大规模的金锑矿床之一, 至今已有一百多年开采历史, 一直以来是该区找矿勘查和科学研究的重点矿床之一(王中雄, 1988; 梁华英, 1989, 1991; 史明魁等, 1994; 鲍肖和陈放, 1995; 康如华, 2002; 吴运军, 2003; 郑时干, 2006; 李己华等, 2007; 刘鹏程等, 2008; 贺文华等, 2015; 张新念, 2016)。尽管在矿区尺度内并没有大规模岩体出露, 但在矿区外围发育着以矿床为中心呈同心圆状分布的多个酸性岩脉群, 并且在龙山金锑矿区的南部还发育曹家坝矽卡岩型钨矿床(张志远等, 2016)。区域物探重力资料也表明, 龙山矿床所在区域存在明显的重力异常(湖南省地质矿产局, 1988)。上述种种迹象表明龙山金锑矿的底部可能存在一定规模的隐伏岩体, 而这些酸性岩脉群很可能就是深部隐伏岩体的地表显示。因此, 许多学者认为岩浆活动与龙山金锑矿成矿可能具有密切的关系, 岩浆活动可能是金锑成矿的热源、流体源和物质来源(鲍肖和陈放, 1995; 郑时干, 2006; 李己华等, 2007; 刘鹏程等, 2008)。但上述认识均基于对矿床研究的推论, 还缺乏岩浆岩的年代学和地球化学的关键证据。本文以龙山金锑矿外围发育的酸性岩脉群为研究对象, 进行了系统的元素地球化学、锆石 U-Pb 年代学和 Hf 同位素地球化学研究, 揭示了岩脉的形成年龄、源区性质及其与龙山金锑矿床的成因联系。

1 地质背景和样品描述

龙山金锑矿位于华南褶皱带的湘中凹陷中部, 东西向白马山-龙山构造隆起带与北东向宁乡-新宁基底断裂带和北西向锡矿山-涟源基底断裂带交汇部位(图 1a)。

矿区位于龙山穹窿的核部, 周边北北东-北东向断裂广

泛发育。矿区主要赋矿地层为震旦系下统江口组上段, 自下而上分四个岩性亚段, 主要为一套浅变质岩系, 岩性为含砾凝灰质砂质板岩、含砾粉砂质板岩、含砾砂质板岩及粉砂质绢云母板岩、浅变质长石英砂岩、浅变质石英砂岩等。其中第一、二岩性段为金锑矿主要赋矿围岩(郑时干, 2006; 贺文华等, 2015)。矿体严格受背斜(含次级背斜)部位的断裂控制, 按其产状可分为 NWW、NNE、NW 和 NE 向四组, 其中 NWW 向组为金锑矿体的主要容矿断裂。按主要金属矿物组合特点, 可将矿石分为三个类型:(1)辉锑矿-毒砂(黄铁矿)-自然金矿石;(2)毒砂-自然金矿石;(3)黄铁矿-自然金矿石。其中以第(1)类型为主(刘鹏程等, 2008)。

酸性岩脉主要以集群出现, 主要发育于龙山隆起的北部及北东缘的柿乡冲、梳装村、砖湾村、枫城里、梧桐村等地, 整体上呈北西向展布。岩脉均填充于寒武系或泥盆系地层中, 通常长达十米、几百米甚至几千米, 大体上呈以龙山金锑矿为心呈扇形分布(图 1b)。柿香村花岗斑岩脉内部还发育石英脉型锑矿化。但由于岩脉露头暴露在地表时间较长, 植被覆盖茂盛, 且当地气候温热, 因此样品大多受较强风化作用(图 2a, b), 蚀变发育硅化、碳酸盐化等。柿香村的花岗斑岩脉部分样品受到矿化影响, 还发育少量黄铁矿化和毒砂化。

野外露头及显微鉴定表明, 岩脉大多为花岗斑岩, 少量为花岗闪长斑岩。样品具有明显的斑状结构和块状构造, 斑晶多为石英、长石, 少量为黑云母等, 副矿物主要有锆石、磷灰石、黑云母、角闪石、榍石等。石英斑晶多为等粒状, 自形程度差, 常具有熔蚀结构, 有时边缘会有反应边(图 2c)。长石斑晶常发育绢云母蚀变, 但保留了不完整的长石假像(图 2d)。黑云母斑晶呈多自形黑云母发生褪色变成白云母, 或蚀变成绿泥石析出大量含铁矿物(图 2e)。

2 测试方法

通过野外地质调察, 分别采集了上述 5 个地区酸性岩脉群的相对新鲜岩石样品, 并经过室内分选, 挑出 5 件样品用于挑选锆石做年龄分析, 16 个岩石样品开展地球化学分析。定年样品经常规重磁方法选出锆石后, 将锆石样品颗粒和锆石标样粘贴在环氧树脂靶上, 然后抛光使其暴露一半晶面。在中国科学院地球化学研究所矿床地球化学国家重点实验室对锆石靶进行透射光、反射光显微照相以及阴极发光图像分析(CL), 以检查锆石的内部结构, 帮助选择适宜的测试点位开展 U-Pb 年代学研究及 Hf 同位素特征分析。

样品的锆石 U-Pb 定年及微量测试在中国科学院地球化学研究所的 LA-ICPMS 实验室完成。详细分析方法见(Liu et al., 2008)。激光剥蚀系统为 GeolasPro, 同位素及微量测试采用 Agilent 7700X ICP-MS。每个时间分辨分析数据包括大约 20 ~ 30s 的空白信号和 50s 的样品信号。采用 ICPMSDataCal 软件对分析数据的离线处理(包括对样品和空白信号的选择、仪器灵敏度漂移校正、元素含量及 U-Th-Pb

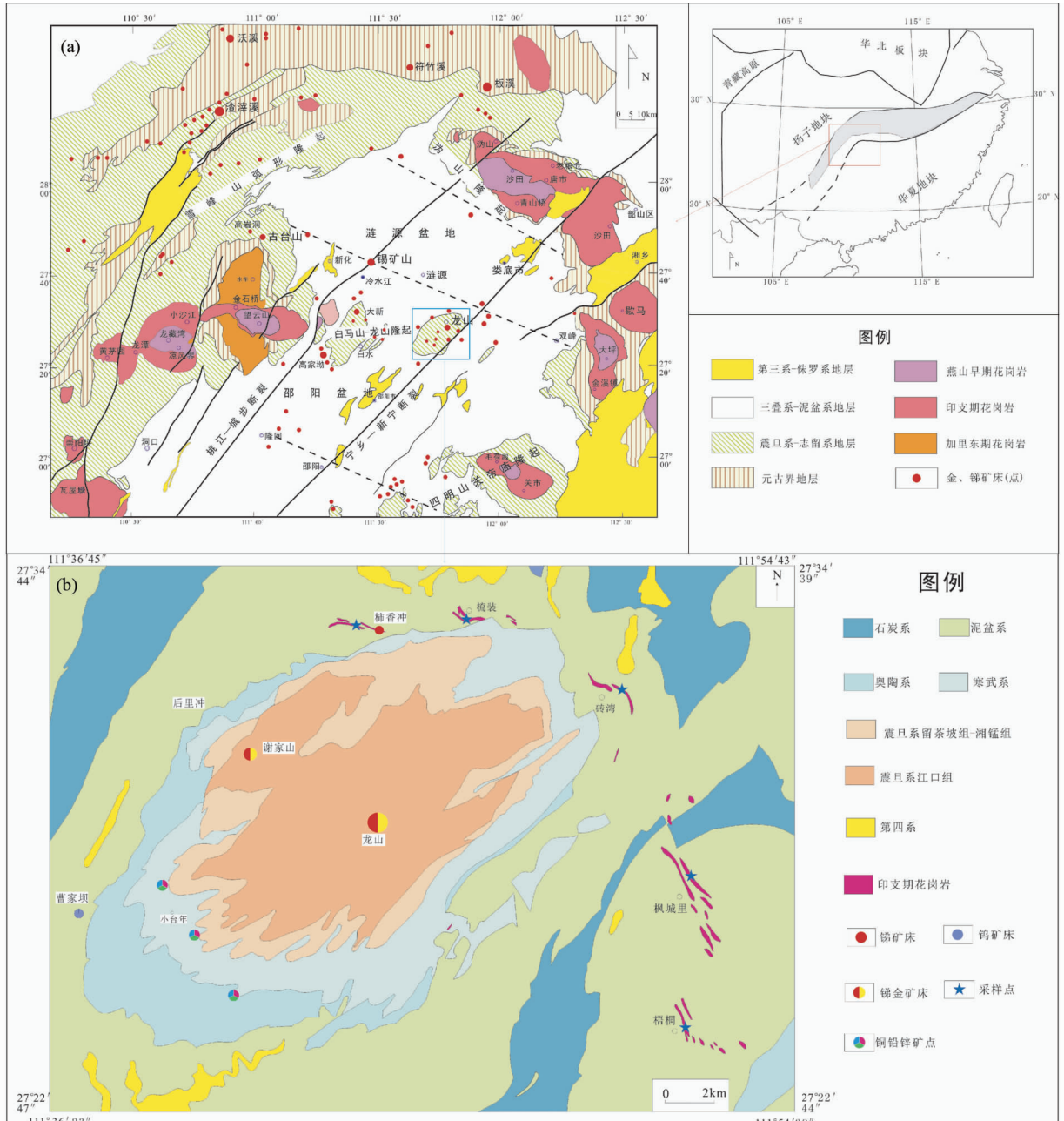


图1 湘中地区地质图 (a, 据陶琰等, 2001; 李已华等, 2007 修改) 和龙山金锑矿区地质图 (b, 据贺文华等, 2015)

Fig. 1 Geological map of Central Hunan Province (a, modified after Tao *et al.*, 2001; Li *et al.*, 2007) and geological map showing Longshan Au-Sb deposit (b, modified after He *et al.*, 2015)

同位素比值和年龄计算) (Liu *et al.*, 2008),详细的仪器操作条件和数据处理方法同(Liu *et al.*, 2008)。锆石微量元素含量利用多个 USGS 参考玻璃(BCR-2G, BIR-1G)作为多外标、Zr 作内标的方法进行定量计算。U-Pb 同位素定年中采用锆石标准 91500 作外标进行同位素分馏校正,每分析 5 个样品点,分析 2 次锆石标样 91500。锆石样品的 U-Pb 年龄谐和图绘制和年龄权重平均计算均采用 Isoplot/Ex-ver3 完成 (Ludwing, 2003)。

锆石的 Lu-Hf 同位素测定在中国地质调查局天津地质

调查中心实验室测试室,利用 MC-LA-ICPMS 完成。该仪器由美国 ESI 公司 NEW WAVE 193nm FX 激光器和美国赛默飞世尔公司 NEPTUNE 多接收等离子质谱组成。其分析方法及仪器参数可参考文献(Hu *et al.*, 2012),采用单点剥蚀模式,斑束固定为 44μm。分析数据的离线处理(包括对样品和空白信号的选择、同位素质量分馏校正)采用软件 ICPMSDataCal 完成。

ε_{Hf} 的计算采用 ^{176}Lu 衰变常数为 $\lambda = 1.867 \times 10^{-11}$



图2 花岗斑岩脉的野外照片(a、b)和显微镜下特征(c、d,正交偏光)

Q-石英;Pl-斜长石;Bi-黑云母

Fig. 2 Field photography of the granite-porphyry dykes (a, b) and micro-photograph of representative samples of the granite-porphyry dykes (c, d, cross-polarized light)

Abbreviations are: Q-quartz; Bi-biotite; Pl-plagioclase

year⁻¹, 球粒陨石现今的(¹⁷⁶Hf/¹⁷⁷Hf)_{CHUR,0} = 0.282772 和 (¹⁷⁶Lu/¹⁷⁷Hf)_{CHUR} = 0.0332 (Blichert-Toft and Albarède, 1997); Hf 亏损地幔模式年龄(t_{DM})的计算采用现今的亏损地幔(¹⁷⁶Hf/¹⁷⁷Hf)_{DM} = 0.28325 和 (¹⁷⁶Lu/¹⁷⁷Hf)_{DM} = 0.0384 (Vervoort and Blichert-Toft, 1999)。由于样品为花岗质岩石, 主要来源于地壳岩石的部分熔融, 所以在计算两阶段模式年龄时, 采用硅铝质大陆地壳的 Lu/Hf 比 $f_{Lu/Hf} = -0.72$ (Amelin *et al.*, 1999; 吴福元等, 2007)。

主量元素和微量元素分析均在中国科学院地球化学研究所矿床地球化学国家重点实验室完成。主量元素采用X-射线荧光法, 仪器型号为 PANalytical AXIOS, 分析误差小于3%。微量元素和稀土元素测试在 PerkinElmer 公司 ELAN DRC-e 型高分辨等离子质谱仪上进行, 精度高于5%。其中成矿元素 Au 含量采用痕量火试法分析, 检测限为 $0.001 \times 10^{-6} \sim 10 \times 10^{-6}$ 。

3 分析结果

3.1 年代学

样品的锆石多呈短柱状, 自形程度较高, 多呈无色。阴极发光图像显示, 锆石晶形完好, 裂纹不发育, 均具有典型岩浆成因锆石的震荡韵环带。所有测试锆石的 Th/U 值为

0.15 ~ 1.18, 且多数样品均在0.4以上(表1), 具有典型岩浆锆石的高 Th/U 值征(Hoskin and Black, 2000; Belousova *et al.*, 2002; Corfu *et al.*, 2003; 吴元保和郑永飞, 2004)。以上特征均表明所测锆石为岩浆成因。因此, 所测的年龄可以代表酸性岩脉的结晶年龄, 分析结果如表1所示。

大部分数据点位于谐和线或附近(图3), 虽然部分分析点不同程度的水平偏离谐和线, 但其分布形式与 Pb 丢失所引起的不谐和明显不同, 而且锆石具有清晰的韵律环带, 表明锆石并未发生 Pb 的丢失, 因此, 可能与²⁰⁷Pb 含量较低较难测定有关(Compston *et al.*, 1992)。

柿香冲花岗斑岩脉进行了14个测试点分析。其中13个测试点显示了较为一致的²⁰⁶Pb/²³⁸U 年龄, 为 223 ~ 212 Ma, 加权平均年龄为 217 ± 1.8 Ma。其中一颗锆石显示与其余锆石明显不同的年龄, 其²⁰⁶Pb/²³⁸U 年龄为 795 Ma, 阴极发光显示具有明显的核边结构, 因此判断为捕获的继承锆石。

梳装花岗岩脉样品也进行了15个测试点分析。所测试的点均显示了较为一致的²⁰⁶Pb/²³⁸U 年龄, 为 223 ~ 216 Ma, 加权平均年龄为 219.7 ± 1.6 Ma。

砖湾花岗岩脉中的锆石成功进行了16个测试点的同位素分析。其中14个测试点显示了较为一致的²⁰⁶Pb/²³⁸U 年龄, 为 224 ~ 214 Ma, 加权平均年龄为 217.1 ± 2.3 Ma, 代表了岩脉的结晶年龄。其中2颗继承锆石显示了较为不一致的

表 1 岩脉的锆石 LA-ICPMS 定年结果

Table 1 LA-ICPMS zircon U-Pb dating of the dykes

| Spot No. | Th/U | $\frac{^{207}\text{Pb}}{^{206}\text{Pb}}$ | 1σ | $\frac{^{207}\text{Pb}}{^{235}\text{U}}$ | 1σ | $\frac{^{206}\text{Pb}}{^{238}\text{U}}$ | 1σ | $\frac{^{207}\text{Pb}}{^{206}\text{Pb}}$ (Ma) | 1σ | $\frac{^{207}\text{Pb}}{^{235}\text{U}}$ | 1σ | $\frac{^{206}\text{Pb}}{^{238}\text{U}}$ | 1σ |
|------------|------|---|-----------|--|-----------|--|-----------|--|-----------|--|-----------|--|-----------|
| 柿香冲 | | | | | | | | | | | | | |
| SXC-02-01 | 0.63 | 0.0493 | 0.0022 | 0.2334 | 0.0102 | 0.0339 | 0.0006 | 167 | 106 | 213 | 8 | 215 | 4 |
| SXC-02-04 | 0.54 | 0.0483 | 0.0019 | 0.2261 | 0.0088 | 0.0336 | 0.0006 | 122 | 93 | 207 | 7 | 213 | 3 |
| SXC-02-05 | 0.41 | 0.0484 | 0.0014 | 0.2342 | 0.0064 | 0.0346 | 0.0004 | 120 | 67 | 214 | 5 | 220 | 2 |
| SXC-02-06 | 0.58 | 0.0512 | 0.0017 | 0.2516 | 0.0083 | 0.0352 | 0.0004 | 254 | 78 | 228 | 7 | 223 | 3 |
| SXC-02-08 | 0.57 | 0.0495 | 0.0028 | 0.2345 | 0.0127 | 0.0346 | 0.0006 | 172 | 131 | 214 | 10 | 219 | 4 |
| SXC-02-09 | 0.56 | 0.0509 | 0.0019 | 0.2391 | 0.0085 | 0.0338 | 0.0005 | 239 | 83 | 218 | 7 | 215 | 3 |
| SXC-02-10 | 0.33 | 0.0515 | 0.0017 | 0.2464 | 0.0078 | 0.0346 | 0.0007 | 261 | 81 | 224 | 6 | 219 | 4 |
| SXC-02-11 | 0.51 | 0.0504 | 0.0018 | 0.2437 | 0.0082 | 0.0347 | 0.0004 | 213 | 81 | 221 | 7 | 220 | 3 |
| SXC-02-12 | 0.48 | 0.0514 | 0.0018 | 0.2395 | 0.0083 | 0.0335 | 0.0004 | 261 | 81 | 218 | 7 | 212 | 3 |
| SXC-02-13 | 0.41 | 0.0517 | 0.0012 | 0.2487 | 0.0057 | 0.0343 | 0.0004 | 272 | 56 | 226 | 5 | 217 | 2 |
| SXC-02-14 | 0.42 | 0.0528 | 0.0019 | 0.2521 | 0.0094 | 0.0341 | 0.0005 | 320 | 116 | 228 | 8 | 216 | 3 |
| SXC-02-15 | 0.35 | 0.0501 | 0.0025 | 0.2321 | 0.0114 | 0.0338 | 0.0004 | 198 | 117 | 212 | 9 | 214 | 2 |
| SXC-02-18 | 0.63 | 0.0510 | 0.0015 | 0.2436 | 0.0071 | 0.0345 | 0.0003 | 243 | 67 | 221 | 6 | 218 | 2 |
| SXC-02-20 | 0.87 | 0.0641 | 0.0019 | 1.1637 | 0.0335 | 0.1313 | 0.0011 | 744 | 63 | 784 | 16 | 795 | 6 |
| 梳装 | | | | | | | | | | | | | |
| SZ-08-04 | 0.65 | 0.0508 | 0.0022 | 0.2437 | 0.0097 | 0.0350 | 0.0006 | 232 | 100 | 221 | 8 | 222 | 4 |
| SZ-08-05 | 0.75 | 0.0464 | 0.0025 | 0.2181 | 0.0120 | 0.0341 | 0.0008 | 20 | 126 | 200 | 10 | 216 | 5 |
| SZ-08-06 | 0.62 | 0.0488 | 0.0020 | 0.2362 | 0.0093 | 0.0348 | 0.0006 | 139 | 94 | 215 | 8 | 221 | 4 |
| SZ-08-07 | 0.69 | 0.0487 | 0.0025 | 0.2360 | 0.0117 | 0.0350 | 0.0006 | 200 | 120 | 215 | 10 | 222 | 4 |
| SZ-08-08 | 0.53 | 0.0534 | 0.0022 | 0.2596 | 0.0103 | 0.0352 | 0.0006 | 346 | 93 | 234 | 8 | 223 | 4 |
| SZ-08-10 | 0.74 | 0.0526 | 0.0027 | 0.2514 | 0.0122 | 0.0347 | 0.0006 | 322 | 119 | 228 | 10 | 220 | 4 |
| SZ-08-13 | 0.46 | 0.0526 | 0.0024 | 0.2529 | 0.0111 | 0.0349 | 0.0005 | 322 | 102 | 229 | 9 | 221 | 3 |
| SZ-08-14 | 0.75 | 0.0506 | 0.0029 | 0.2400 | 0.0137 | 0.0345 | 0.0004 | 220 | 133 | 218 | 11 | 219 | 3 |
| SZ-08-15 | 0.87 | 0.0516 | 0.0031 | 0.2432 | 0.0137 | 0.0347 | 0.0004 | 265 | 137 | 221 | 11 | 220 | 3 |
| SZ-08-16 | 0.66 | 0.0506 | 0.0023 | 0.2432 | 0.0112 | 0.0350 | 0.0004 | 233 | 103 | 221 | 9 | 222 | 3 |
| SZ-08-19 | 0.48 | 0.0503 | 0.0032 | 0.2380 | 0.0152 | 0.0344 | 0.0005 | 209 | 144 | 217 | 12 | 218 | 3 |
| SZ-08-20 | 1.01 | 0.0514 | 0.0027 | 0.2478 | 0.0128 | 0.0349 | 0.0004 | 261 | 88 | 225 | 10 | 221 | 3 |
| SZ-08-11 | 0.59 | 0.0506 | 0.0024 | 0.2420 | 0.0108 | 0.0348 | 0.0004 | 233 | 103 | 220 | 9 | 221 | 3 |
| SZ-08-24 | 0.61 | 0.0513 | 0.0017 | 0.2438 | 0.0080 | 0.0343 | 0.0003 | 254 | 76 | 222 | 7 | 217 | 2 |
| SZ-08-25 | 0.87 | 0.0521 | 0.0044 | 0.2435 | 0.0202 | 0.0340 | 0.0006 | 287 | 196 | 221 | 17 | 216 | 4 |
| 砖湾 | | | | | | | | | | | | | |
| ZW-01-03 | 0.31 | 0.0566 | 0.0029 | 0.2697 | 0.0132 | 0.0345 | 0.0006 | 476 | 110 | 242 | 11 | 219 | 4 |
| ZW-01-04 | 0.54 | 0.0486 | 0.0024 | 0.2277 | 0.0107 | 0.0339 | 0.0005 | 128 | 113 | 208 | 9 | 215 | 3 |
| ZW-01-05 | 0.53 | 0.0543 | 0.0035 | 0.2575 | 0.0153 | 0.0354 | 0.0007 | 387 | 144 | 233 | 12 | 224 | 4 |
| ZW-01-06 | 0.56 | 0.0576 | 0.0030 | 0.2764 | 0.0134 | 0.0353 | 0.0005 | 522 | 119 | 248 | 11 | 224 | 3 |
| ZW-01-07 | 0.50 | 0.0658 | 0.0031 | 1.0919 | 0.0537 | 0.1195 | 0.0017 | 1200 | 100 | 749 | 26 | 728 | 10 |
| ZW-01-08 | 0.86 | 0.0510 | 0.0032 | 0.2368 | 0.0145 | 0.0346 | 0.0006 | 239 | 138 | 216 | 12 | 219 | 4 |
| ZW-01-09 | 0.50 | 0.0503 | 0.0027 | 0.2302 | 0.0119 | 0.0337 | 0.0007 | 206 | 122 | 210 | 10 | 214 | 4 |
| ZW-01-10 | 0.47 | 0.0564 | 0.0036 | 0.2694 | 0.0164 | 0.0346 | 0.0006 | 465 | 147 | 242 | 13 | 219 | 4 |
| ZW-01-12 | 0.44 | 0.0511 | 0.0021 | 0.2457 | 0.0103 | 0.0346 | 0.0005 | 256 | 96 | 223 | 8 | 220 | 3 |
| ZW-01-13 | 0.51 | 0.0509 | 0.0028 | 0.2380 | 0.0119 | 0.0343 | 0.0006 | 235 | 132 | 217 | 10 | 217 | 4 |
| ZW-01-14 | 0.56 | 0.0493 | 0.0025 | 0.2266 | 0.0108 | 0.0334 | 0.0005 | 165 | 117 | 207 | 9 | 212 | 3 |
| ZW-01-15 | 0.88 | 0.0627 | 0.0013 | 0.8862 | 0.0196 | 0.1021 | 0.0011 | 698 | 46 | 644 | 11 | 627 | 7 |
| ZW-01-17 | 0.49 | 0.0620 | 0.0013 | 0.2972 | 0.0065 | 0.0348 | 0.0004 | 672 | 44 | 264 | 5 | 220 | 2 |
| ZW-01-19 | 0.44 | 0.0509 | 0.0009 | 0.2422 | 0.0045 | 0.0344 | 0.0003 | 235 | 44 | 220 | 4 | 218 | 2 |
| ZW-01-20 | 0.54 | 0.0505 | 0.0015 | 0.2369 | 0.0067 | 0.0341 | 0.0004 | 220 | 67 | 216 | 5 | 216 | 2 |
| ZW-01-22 | 1.18 | 0.0536 | 0.0014 | 0.2459 | 0.0059 | 0.0333 | 0.0003 | 354 | 57 | 223 | 5 | 211 | 2 |
| 枫城里 | | | | | | | | | | | | | |
| FC-05-01 | 0.31 | 0.0508 | 0.0017 | 0.2438 | 0.0083 | 0.0346 | 0.0003 | 232 | 78 | 222 | 7 | 220 | 2 |
| FC-05-02 | 0.38 | 0.0528 | 0.0025 | 0.2543 | 0.0117 | 0.0351 | 0.0004 | 320 | 109 | 230 | 9 | 222 | 3 |

续表 1

Continued Table 1

| Spot No. | Th/U | $\frac{^{207}\text{Pb}}{^{206}\text{Pb}}$ | 1 σ | $\frac{^{207}\text{Pb}}{^{235}\text{U}}$ | 1 σ | $\frac{^{206}\text{Pb}}{^{238}\text{U}}$ | 1 σ | $\frac{^{207}\text{Pb}}{^{206}\text{Pb}}$ (Ma) | 1 σ | $\frac{^{207}\text{Pb}}{^{235}\text{U}}$ | 1 σ | $\frac{^{206}\text{Pb}}{^{238}\text{U}}$ | 1 σ |
|-----------|------|---|------------|--|------------|--|------------|---|------------|--|------------|--|------------|
| FC-05-04 | 0.52 | 0.0506 | 0.0036 | 0.2451 | 0.0176 | 0.0351 | 0.0005 | 220 | 160 | 223 | 14 | 222 | 3 |
| FC-05-05 | 0.76 | 0.0527 | 0.0023 | 0.2524 | 0.0108 | 0.0348 | 0.0004 | 317 | 100 | 229 | 9 | 220 | 2 |
| FC-05-08 | 0.47 | 0.0507 | 0.0026 | 0.2431 | 0.0124 | 0.0348 | 0.0004 | 228 | 119 | 221 | 10 | 220 | 3 |
| FC-05-11 | 0.32 | 0.0513 | 0.0028 | 0.2428 | 0.0128 | 0.0345 | 0.0004 | 257 | 126 | 221 | 10 | 219 | 3 |
| FC-05-12 | 0.63 | 0.0492 | 0.0017 | 0.2304 | 0.0077 | 0.0344 | 0.0005 | 167 | 81 | 211 | 6 | 218 | 3 |
| FC-05-14 | 0.87 | 0.0491 | 0.0019 | 0.2288 | 0.0082 | 0.0342 | 0.0006 | 154 | 93 | 209 | 7 | 217 | 3 |
| FC-05-17 | 0.47 | 0.0521 | 0.0042 | 0.2393 | 0.0185 | 0.0343 | 0.0005 | 287 | 181 | 218 | 15 | 217 | 3 |
| FC-05-19 | 0.77 | 0.0498 | 0.0012 | 0.2382 | 0.0056 | 0.0346 | 0.0003 | 187 | 57 | 217 | 5 | 219 | 2 |
| 梧桐 | | | | | | | | | | | | | |
| WTC-10-01 | 0.32 | 0.0513 | 0.0014 | 0.2406 | 0.0068 | 0.0341 | 0.0005 | 254 | 63 | 219 | 6 | 216 | 3 |
| WTC-10-02 | 0.55 | 0.0509 | 0.0017 | 0.2425 | 0.0088 | 0.0346 | 0.0006 | 235 | 78 | 220 | 7 | 219 | 4 |
| WTC-10-03 | 0.60 | 0.0588 | 0.0014 | 0.2830 | 0.0064 | 0.0348 | 0.0002 | 561 | 52 | 253 | 5 | 221 | 1 |
| WTC-10-05 | 0.62 | 0.0500 | 0.0012 | 0.2443 | 0.0047 | 0.0344 | 0.0003 | 195 | 28 | 222 | 4 | 218 | 2 |
| WTC-10-06 | 0.69 | 0.0670 | 0.0049 | 1.1880 | 0.0843 | 0.1281 | 0.0040 | 839 | 152 | 795 | 39 | 777 | 23 |
| WTC-10-07 | 0.56 | 0.0510 | 0.0010 | 0.2402 | 0.0048 | 0.0342 | 0.0003 | 243 | 46 | 219 | 4 | 217 | 2 |
| WTC-10-10 | 0.52 | 0.0519 | 0.0009 | 0.2459 | 0.0046 | 0.0343 | 0.0003 | 280 | 41 | 223 | 4 | 217 | 2 |
| WTC-10-12 | 0.58 | 0.0560 | 0.0013 | 0.2649 | 0.0060 | 0.0344 | 0.0003 | 450 | 52 | 239 | 5 | 218 | 2 |
| WTC-10-13 | 0.15 | 0.0670 | 0.0009 | 1.1261 | 0.0163 | 0.1212 | 0.0010 | 839 | 33 | 766 | 8 | 738 | 6 |
| WTC-10-14 | 0.33 | 0.0493 | 0.0025 | 0.2327 | 0.0117 | 0.0341 | 0.0004 | 161 | 117 | 212 | 10 | 216 | 2 |
| WTC-10-16 | 0.59 | 0.0539 | 0.0017 | 0.2487 | 0.0074 | 0.0335 | 0.0004 | 365 | 69 | 225 | 6 | 212 | 3 |
| WTC-10-17 | 0.63 | 0.0553 | 0.0015 | 0.2561 | 0.0069 | 0.0335 | 0.0004 | 433 | 59 | 231 | 6 | 212 | 2 |
| WTC-10-20 | 0.49 | 0.0508 | 0.0014 | 0.2368 | 0.0067 | 0.0336 | 0.0003 | 232 | 63 | 216 | 5 | 213 | 2 |

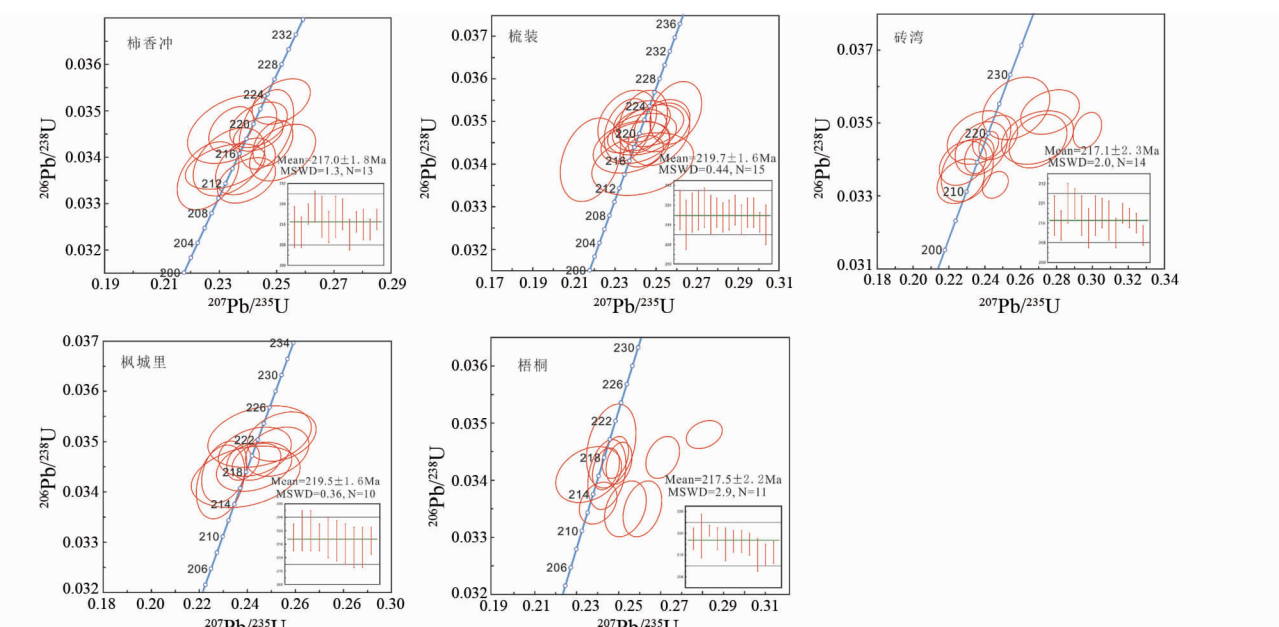


图3 岩脉的锆石U-Pb谐和图

Fig. 3 U-Pb concordia diagrams of zircons from the dykes

年龄, 其 $^{206}\text{Pb}/^{238}\text{U}$ 年龄分别为728 Ma、627 Ma。

枫城里岩脉样品也进行了10个测试点分析。显示了较为一致的 $^{206}\text{Pb}/^{238}\text{U}$ 年龄, 为217~220 Ma, 加权平均年龄为

219.5 ± 1.6 Ma

梧桐村花岗闪长岩脉样品也进行了13个测试点分析。其中11个测试点显示了较为一致的 $^{206}\text{Pb}/^{238}\text{U}$ 年龄, 为221

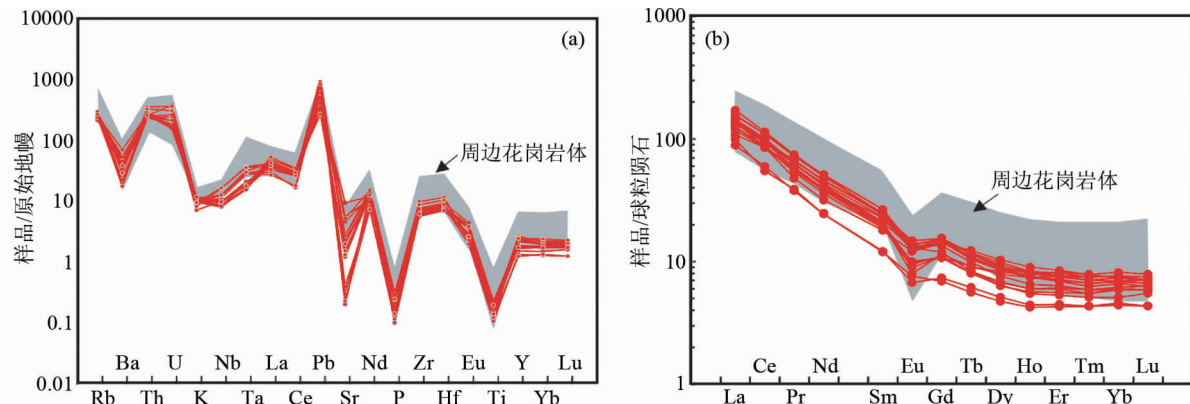


图 4 脉岩的原始地幔标准化微量元素蛛网图(a, 标准化值据 Sun and McDonough, 1989) 和球粒陨石标准化稀土元素分布型图(b, 标准化值据 Taylor and McLennan, 1985)

周边花岗岩体数据来源:关帝庙(柏道远等,2014;赵增霞等,2015),白马山(陈卫锋等,2007;Fu et al., 2015);沩山(Fu et al., 2015),紫云山(刘凯等,2014)

Fig. 4 Primitive mantle-normalized spider diagram (a, normalization values after Sun and McDonough, 1989) and chondrite-normalized REE pattern diagram (a, normalization values after Taylor and McLennan, 1985) of dykes

The data of the plutons from: Guandimiao (Bai et al., 2014; Zhao et al., 2015); Baimashan (Chen et al., 2007; Fu et al., 2015); Weishan (Fu et al., 2015); Ziyunshan (Liu et al., 2014)

~212Ma, 加权平均年龄为 217.5 ± 2.2 Ma。其中 2 颗继承锆石显示了较为不一致的年龄, 其 $^{206}\text{Pb}/^{238}\text{U}$ 年龄分别为 777Ma, 738Ma。

可以看出, 龙山矿床周边出露的花岗斑岩脉显示了较为一致的年龄, 表明它们应该是一次岩浆活动侵入的产物, 其结晶年龄为 220~217Ma。5 颗继承锆石的年龄均分布在谐和线上, 其年龄为 795~627Ma, 暗示其形成过程中有少量新元古代物质加入。

3.2 地球化学特征

表 2 列出了岩脉样品的主要元素分析结果。从表中可以看出, 岩脉样品具有很高的硅含量 ($\text{SiO}_2 = 70.21\% \sim 76.15\%$), 高的烧失量和 ACNK 值 ($\text{LOI} = 3 \sim 5.58\%$, $\text{ACNK} = 1.67 \sim 5.14$), 以及低的钠 ($\text{Na}_2\text{O} = 0.03\% \sim 3.20\%$, 平均为 0.29%)、钙 ($\text{CaO} = 0.01\% \sim 2.51\%$, 平均为 0.23%) 和镁 ($\text{MgO} = 0.2\% \sim 1.26\%$, 平均为 0.47%) 元素等。这些特征可能与岩石样品受到了较强的蚀变作用有关。因此, 在这种条件下岩脉样品的主要元素受到了较大干扰, 其代表性存疑。

热液蚀变作用也会影响岩石中微量元素的含量变化。但一般认为高场强元素和稀土元素具有较弱的活泼性, 它们受热液蚀变的影响较弱(Jiang et al., 2005)。样品的微量元素及稀土元素分析结果如表 2 所示。为了便于判断蚀变作用对岩石微量元素及稀土元素的影响, 我们收集了湘中盆地周边出露的印支晚期的岩体(白马山岩体、关帝庙岩体、沩山岩体、紫云山岩体)进行对比, 其微量元素原始地幔蛛网图和稀土元素含量蛛网图如图 4 所示。

微量元素上, 除少数元素(Sr、P)可能受到不同程度蚀变

的影响而导致其含量有较大变化外, 其余元素含量较为均匀。微量元素原始地幔标准化图解上(图 4a), 岩脉的微量元素特征与周边同期花岗岩相似, 均表现为富集大离子亲石元素 Rb、Th、U 和 Pb, 而亏损高场强元素 Nb、Ta、Ti 和 P、Sr、Ba 等, 这些特征与南岭东段强过铝质花岗岩相似(孙涛等, 2003)。其中 Sr、P、Ti 的亏损可能是由于斜长石、磷灰石和金红石等矿物的分离结晶所致。

在球粒陨石标准化稀土配分图, 岩脉与同期花岗岩体同样具有相似的稀土元素特征(图 4b), 均具有较低的稀土元素总量($\Sigma\text{REE} = 79.2 \times 10^{-6} \sim 153.3 \times 10^{-6}$); 轻重稀土分馏明显, 具有明显右倾的稀土配分模式($\text{La/Yb})_N = 14.8 \sim 28.8$); 轻稀土的分馏程度相对($\text{La/Sm})_N = 5.2 \sim 8.2$, 而重稀土分馏相对不明显($\text{Gd/Yb})_N = 1.3 \sim 2.3$; 明显的 Eu 负异常, $\delta\text{Eu} = 0.5 \sim 0.8$, 暗示岩浆形成过程中可能经历了比较强烈的分离结晶作用或源区有斜长石的残留。

3.3 锆石的稀土元素特征

锆石的稀土元素含量 $\Sigma\text{REE} = 598.2 \times 10^{-6} \sim 1653 \times 10^{-6}$ 之间, 轻稀土含量为 $9.1 \times 10^{-6} \sim 77.4 \times 10^{-6}$ (见电子版附表 1), 个别测点的轻稀土含量较高, 可能是由于测点含有磷灰石矿物包体所致(吴元保和郑永飞, 2004; 关俊雷等, 2014)。重稀土的含量较高, 为 $586 \times 10^{-6} \sim 1618 \times 10^{-6}$ 。且表现出明显的左倾。锆石中的稀土元素具有明显的 Ce 正异常和 Eu 负异常(图 5), 这种特点与典型的壳源岩浆锆石中的稀土元素组成特征是一致, 暗示其岩浆主要由壳源物质部分熔融而来(Miller and White, 1998; Hoskin and Schaltegger, 2003; Hanchar and van Westrenen, 2007)。

表2 岩脉的主要元素(wt%)和微量元素($\times 10^{-6}$)含量Table 2 Major (wt%) and trace element ($\times 10^{-6}$) data of the dykes

| 样品号 | 地区 | | 柿香冲 | | 梳装 | | 砖弯 | | 枫城里 | | 梧桐 | | | | | |
|--------------------------------|--------|--------|--------|--------|--------|--------|--------|--------|--------|--------|--------|--------|--------|--------|--------|--------|
| | SXC-01 | SXC-02 | SXC-03 | SZ-05 | SZ-07 | SZ-08 | ZW-01 | ZW-02 | ZW-03 | ZW-04 | FC-02 | FC-05 | FC-06 | WTC-08 | WTC-09 | WTC-10 |
| SiO ₂ | 75.82 | 70.21 | 74.92 | 75.12 | 72.10 | 71.78 | 74.93 | 72.15 | 74.22 | 73.19 | 73.90 | 76.15 | 73.03 | 73.57 | 72.55 | 73.63 |
| Al ₂ O ₃ | 14.84 | 13.96 | 13.84 | 15.35 | 15.56 | 15.29 | 15.11 | 15.68 | 15.52 | 15.76 | 15.19 | 13.47 | 15.19 | 14.83 | 16.40 | 16.37 |
| Fe ₂ O ₃ | 1.59 | 2.48 | 2.50 | 1.22 | 3.01 | 2.80 | 1.44 | 3.20 | 1.27 | 2.23 | 1.97 | 1.79 | 2.18 | 1.97 | 2.38 | 1.70 |
| MgO | 0.23 | 1.26 | 0.33 | 0.20 | 0.27 | 0.25 | 0.23 | 0.29 | 0.27 | 0.27 | 0.65 | 0.39 | 1.06 | 1.26 | 0.35 | 0.28 |
| CaO | 0.01 | 2.51 | 0.02 | 0.14 | 0.25 | 0.01 | 0.02 | 0.13 | 0.04 | 0.05 | 0.15 | 0.14 | 0.04 | 0.02 | 0.05 | |
| Na ₂ O | 0.07 | 0.11 | 0.06 | 0.10 | 0.58 | 3.20 | 0.07 | 0.07 | 0.09 | 0.08 | 0.05 | 0.04 | 0.06 | 0.04 | 0.03 | 0.03 |
| K ₂ O | 3.68 | 3.33 | 3.34 | 3.74 | 3.56 | 2.48 | 3.98 | 4.00 | 4.05 | 4.10 | 3.82 | 3.29 | 3.45 | 3.24 | 2.87 | 3.30 |
| TiO ₂ | 0.31 | 0.29 | 0.29 | 0.33 | 0.37 | 0.42 | 0.33 | 0.43 | 0.36 | 0.38 | 0.22 | 0.20 | 0.25 | 0.23 | 0.29 | 0.26 |
| P ₂ O ₅ | 0.059 | 0.075 | 0.046 | 0.038 | 0.083 | 0.070 | 0.027 | 0.039 | 0.038 | 0.066 | 0.046 | 0.044 | 0.063 | 0.031 | 0.078 | 0.065 |
| MnO | 0.01 | 0.05 | 0.01 | 0.01 | 0.07 | 0.03 | 0.01 | 0.01 | 0.01 | 0.03 | 0.01 | 0.03 | 0.02 | 0.01 | 0.01 | 0.00 |
| LOI | 3.40 | 5.58 | 3.87 | 3.72 | 4.19 | 3.00 | 3.34 | 4.13 | 3.49 | 3.81 | 4.11 | 3.54 | 4.44 | 4.44 | 4.91 | 4.23 |
| Total | 100.10 | 99.92 | 99.27 | 99.87 | 99.99 | 99.63 | 99.50 | 100.05 | 99.48 | 100.00 | 100.05 | 99.10 | 99.92 | 99.69 | 99.90 | 99.95 |
| ACNK | 3.60 | 1.67 | 3.69 | 3.61 | 3.07 | 1.82 | 3.40 | 3.50 | 3.25 | 3.39 | 3.53 | 3.45 | 3.72 | 4.07 | 5.14 | 4.41 |
| Au | 0.002 | <0.001 | <0.001 | <0.001 | <0.001 | <0.001 | <0.001 | <0.001 | <0.001 | <0.001 | <0.001 | <0.001 | <0.001 | <0.001 | <0.001 | <0.001 |
| Sb | 35.4 | 27.2 | 41.9 | 2.1 | 1.6 | 1.7 | 0.9 | 1.9 | 2.0 | 2.4 | 0.7 | 1.4 | 0.7 | 2.5 | 3.0 | 2.5 |
| Cr | 20 | 20 | 19 | 22 | 22 | 46 | 20 | 25 | 24 | 24 | 12 | 14 | 15 | 12 | 11 | 10 |
| As | 538 | 975 | 5540 | 238 | 29.8 | 15.5 | 62.9 | 185.5 | 221 | 258 | 7.7 | 34.1 | 6.1 | 7.2 | 375 | 136.5 |
| Rb | 177.5 | 161.5 | 164.0 | 177.0 | 174.5 | 148.0 | 175.5 | 188.0 | 185.0 | 199.5 | 198.5 | 163.5 | 187.5 | 190.0 | 188.5 | 206 |
| Sr | 112.5 | 229 | 138.5 | 67.9 | 67.4 | 129.0 | 32.2 | 30.6 | 49.5 | 33.0 | 5.2 | 10.2 | 7.7 | 5.9 | 58.4 | 38.2 |
| Zr | 77.7 | 72.5 | 75.3 | 81.9 | 84.6 | 87.7 | 76.1 | 75.5 | 79.8 | 77.2 | 99.1 | 89.0 | 92.4 | 95.2 | 126.5 | 113.0 |
| Nb | 7.0 | 8.1 | 6.6 | 7.0 | 6.8 | 8.3 | 7.8 | 8.3 | 8.0 | 8.2 | 10.4 | 9.2 | 10.0 | 10.3 | 13.2 | 13.4 |
| Cs | 18.1 | 27.2 | 16.3 | 51.0 | 47.2 | 31.7 | 15.3 | 19.3 | 19.1 | 22.6 | 13.5 | 7.7 | 12.6 | 7.9 | 11.6 | 9.5 |
| Ba | 430 | 340 | 320 | 250 | 550 | 420 | 280 | 300 | 360 | 170 | 150 | 180 | 140 | 140 | 140 | 230 |
| La | 31.8 | 28.0 | 29.7 | 31.4 | 36.6 | 37.2 | 33.9 | 34.2 | 33.0 | 40.6 | 32.4 | 23.5 | 25.6 | 21.0 | 32.4 | 29.6 |
| Ce | 57.6 | 52.0 | 52.8 | 58.3 | 67.2 | 66.8 | 58.8 | 61.6 | 59.2 | 69.8 | 56.2 | 33.6 | 52.0 | 36.5 | 52.9 | 52.9 |

续表 2
Continued Table 2

| 样品号 | 地区 | | 柿香冲 | | 梳装 | | 砖湾 | | 枫城里 | | 梧桐 | | | | | |
|----------------------|--------|--------|--------|-------|-------|-------|-------|-------|-------|-------|-------|-------|-------|--------|--------|--------|
| | SXC-01 | SXC-02 | SXC-03 | SZ-05 | SZ-07 | SZ-08 | ZW-01 | ZW-02 | ZW-03 | ZW-04 | FC-02 | FC-05 | FC-06 | WTC-08 | WTC-09 | WTC-10 |
| Pr | 5.5 | 5.4 | 5.1 | 5.9 | 6.9 | 6.3 | 6.0 | 5.9 | 7.1 | 6.3 | 3.7 | 4.5 | 3.6 | 5.6 | 5.3 | |
| Nd | 18.4 | 18.4 | 16.7 | 20.2 | 23.9 | 23.1 | 21.5 | 19.4 | 19.6 | 23.5 | 21.3 | 11.4 | 14.8 | 11.4 | 18.1 | 17.7 |
| Sm | 3.2 | 3.5 | 2.9 | 3.5 | 4.1 | 3.8 | 3.8 | 3.0 | 3.2 | 3.7 | 3.7 | 1.9 | 2.8 | 1.8 | 3.1 | 2.9 |
| Eu | 0.6 | 0.7 | 0.6 | 0.7 | 0.8 | 0.7 | 0.6 | 0.6 | 0.8 | 0.8 | 0.9 | 0.4 | 0.7 | 0.4 | 0.5 | 0.5 |
| Gd | 2.3 | 3.0 | 2.2 | 3.0 | 3.2 | 3.0 | 3.1 | 2.2 | 2.5 | 2.8 | 3.2 | 1.5 | 2.9 | 1.4 | 2.4 | 2.2 |
| Tb | 0.3 | 0.4 | 0.3 | 0.4 | 0.4 | 0.4 | 0.4 | 0.3 | 0.3 | 0.4 | 0.4 | 0.2 | 0.5 | 0.2 | 0.3 | 0.3 |
| Dy | 1.6 | 2.2 | 1.7 | 2.2 | 2.3 | 2.2 | 2.4 | 1.6 | 1.7 | 1.9 | 2.5 | 1.3 | 2.6 | 1.2 | 2.0 | 2.1 |
| Ho | 0.3 | 0.4 | 0.3 | 0.4 | 0.5 | 0.4 | 0.5 | 0.3 | 0.3 | 0.4 | 0.5 | 0.3 | 0.5 | 0.2 | 0.4 | 0.4 |
| Er | 0.9 | 1.2 | 1.0 | 1.1 | 1.2 | 1.2 | 1.3 | 0.9 | 1.0 | 1.1 | 1.3 | 0.7 | 1.4 | 0.7 | 1.3 | 1.4 |
| Tm | 0.1 | 0.2 | 0.2 | 0.2 | 0.2 | 0.2 | 0.2 | 0.1 | 0.1 | 0.1 | 0.2 | 0.1 | 0.2 | 0.1 | 0.2 | 0.2 |
| Yb | 1.0 | 1.2 | 1.1 | 1.1 | 1.2 | 1.2 | 1.3 | 0.9 | 1.0 | 1.0 | 1.3 | 0.8 | 1.2 | 0.8 | 1.3 | 1.4 |
| Lu | 0.2 | 0.2 | 0.2 | 0.2 | 0.2 | 0.2 | 0.2 | 0.1 | 0.2 | 0.2 | 0.2 | 0.1 | 0.2 | 0.1 | 0.2 | 0.2 |
| Y | 8.9 | 12.2 | 9.7 | 11.9 | 12.7 | 11.4 | 13.9 | 8.2 | 9.3 | 10.2 | 12.8 | 7.2 | 14.2 | 6.7 | 13.6 | 13.1 |
| Hf | 2.6 | 2.5 | 2.5 | 2.7 | 2.7 | 2.8 | 2.5 | 2.5 | 2.5 | 2.6 | 3.3 | 2.9 | 3.0 | 3.1 | 4.1 | 3.7 |
| Ta | 0.9 | 1.0 | 0.8 | 0.8 | 0.7 | 0.9 | 0.9 | 0.8 | 0.8 | 0.9 | 1.5 | 1.3 | 1.3 | 1.4 | 1.7 | 1.7 |
| Pb | 44.8 | 26.2 | 37.3 | 33.8 | 39.3 | 37.3 | 27.4 | 26.6 | 20.8 | 46.8 | 60.7 | 52.6 | 52.8 | 45.3 | 83.5 | 63.5 |
| Th | 23.7 | 21.8 | 23.7 | 24.5 | 24.7 | 23.7 | 25.1 | 24.0 | 26.2 | 23.7 | 21.3 | 23.2 | 22.5 | 32.6 | 30.3 | |
| U | 3.7 | 4.3 | 3.8 | 4.2 | 4.0 | 4.7 | 3.9 | 4.0 | 3.6 | 4.7 | 8.6 | 5.6 | 6.0 | 4.9 | 8.3 | 7.0 |
| ΣREE | 123.8 | 116.7 | 114.7 | 128.6 | 148.6 | 147.4 | 134.3 | 131.3 | 128.8 | 153.3 | 130.3 | 79.4 | 109.9 | 79.5 | 120.6 | 117.2 |
| LREE | 117.1 | 107.9 | 107.7 | 120.1 | 139.4 | 138.6 | 125.1 | 124.8 | 121.7 | 145.5 | 120.8 | 74.4 | 100.4 | 74.8 | 112.5 | 109.0 |
| HREE | 6.8 | 8.7 | 6.9 | 8.5 | 9.1 | 8.8 | 9.3 | 6.5 | 7.1 | 7.8 | 9.6 | 5.0 | 9.5 | 4.8 | 8.1 | 8.3 |
| LREE/HREE | 17.3 | 12.4 | 15.6 | 14.1 | 15.3 | 15.8 | 13.5 | 19.2 | 17.1 | 18.7 | 12.6 | 14.9 | 10.6 | 15.6 | 14.0 | 13.2 |
| (La/Yb) _N | 22.4 | 17.3 | 20.3 | 20.1 | 22.2 | 23.0 | 19.5 | 28.2 | 23.7 | 28.8 | 17.9 | 22.5 | 14.8 | 19.3 | 18.0 | 15.3 |
| (La/Sn) _N | 6.5 | 5.2 | 6.7 | 5.7 | 6.3 | 5.8 | 7.4 | 7.1 | 5.7 | 8.2 | 6.0 | 7.4 | 6.7 | 6.5 | 6.7 | 6.7 |
| (Gd/Yb) _N | 1.8 | 2.1 | 1.7 | 2.2 | 2.2 | 2.1 | 2.1 | 2.3 | 2.0 | 1.7 | 1.9 | 1.5 | 1.5 | 1.3 | 2.0 | 2.0 |
| δEu | 0.6 | 0.7 | 0.7 | 0.7 | 0.7 | 0.7 | 0.7 | 0.7 | 0.7 | 0.8 | 0.7 | 0.8 | 0.7 | 0.8 | 0.5 | 0.6 |

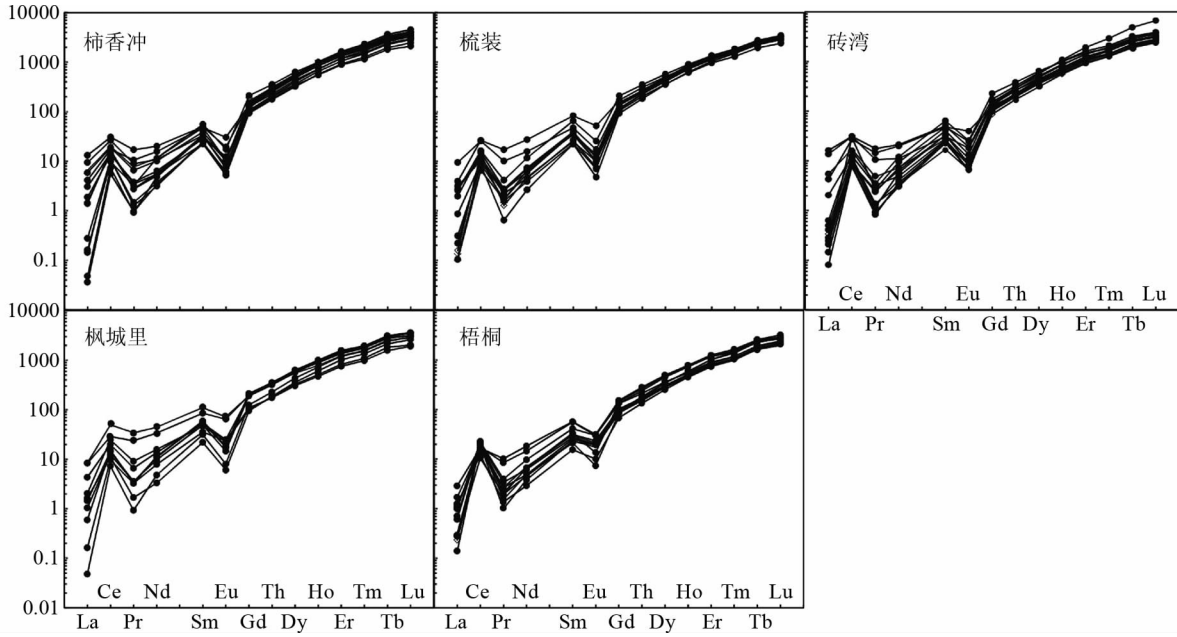


图5 岩脉中锆石的球粒陨石标准化稀土元素分布型式图(标准化值据 Taylor and McLennan, 1985)

Fig. 5 Chondrite-normalized REE pattern diagrams of zircons from dykes (normalization values after Taylor and McLennan, 1985)

3.4 Hf 同位素特征

样品的 Hf 同位素组成分析结果如表 3 所示, 其 $\varepsilon_{\text{Hf}}(t)$ 值及模式年龄计算均采用本研究取得的 U-Pb 年龄。样品所测锆石的 $^{176}\text{Lu}/^{177}\text{Hf}$ 比值均小于 0.002, 表明锆石在形成后具有极低的放射性成因 Hf 积累, 因此所测定的 $^{176}\text{Hf}/^{177}\text{Hf}$ 比值基本可以代表锆石结晶时体系的 Hf 同位素组成 (Amelin *et al.*, 1999; 吴福元等, 2007)。所测锆石的 $f_{\text{Lu/Hf}}$ 值在 $-0.99 \sim -0.95$ 之间, 远低于镁铁质下地壳 (-0.34 ; Amelin *et al.*, 1999) 和硅铝质地壳 (-0.72 ; Vervoort *et al.*, 1996) 的值。因此锆石的 Hf 同位素的二阶段模式年龄 (t_{DM2}) 代表源区物质从地幔分离的时间。

不同地区的岩脉中锆石均显示出较为均一的 Hf 同位素组成, 其 $^{176}\text{Hf}/^{177}\text{Hf}$ 比值为 $0.282264 \sim 0.282536$, $\varepsilon_{\text{Hf}}(t) = -13.4 \sim -3.7$ 。 t_{DM2} 为 $2089 \sim 1482\text{Ma}$ 。对其中的继承锆石也进行了 Hf 同位素研究, 其组成也较为均一, $^{176}\text{Hf}/^{177}\text{Hf}$ 比值为 $0.281941 \sim 0.282134$, $\varepsilon_{\text{Hf}}(t) = -14.3 \sim -6.9$ 。 t_{DM2} 为 $2451 \sim 2072\text{Ma}$ 。

4 讨论

4.1 岩脉的形成时代

前人对该地区的花岗斑岩脉开展过少量定年工作, 其结果显示梧桐村和枫城里地区的花岗闪长斑岩脉年龄为 157Ma 左右 (湖南省地质矿产局, 1988), 属于燕山期岩体, 但其所测得到硅含量数据异常高 ($\text{SiO}_2 = 70\% \sim 78\%$), 暗示

所分析的样品已受到较强的硅化等蚀变影响, 因此当时所测年龄可能会受到蚀变的较大干扰。

锆石由于分布广泛, 抗风化能力强等因素, 成为 U-Pb 同位素体系中最合适定年的矿物, 在地质学中得到了广泛应用。本次开展的锆石 LA-ICPMS U-Pb 年代学研究显示, 柿香冲等五处酸性岩脉均显示具有较为一致的锆石 U-Pb 年龄, 为 $220 \sim 217\text{Ma}$, 与湘中盆地周边的花岗岩如白马山岩体 ($216 \sim 210\text{Ma}$, 李建华等, 2014; Fu *et al.*, 2015)、紫云山岩体 ($223 \sim 220\text{Ma}$, 刘凯等, 2014; Fu *et al.*, 2015)、沩山岩体 ($218 \sim 214\text{Ma}$, 丁兴等, 2005, 2012; Fu *et al.*, 2015)、关帝庙岩体 (222Ma , 赵增霞等, 2015) 等具有一致的成岩年龄。同时地球化学特征表明, 区内酸性岩脉与周边花岗岩体具有相似的微量元素特征及源区特征, 暗示龙山地区酸性岩脉与湘中周边的印支晚期岩体具有成因联系, 可能为相似构造背景下的同一次岩浆活动的产物。

4.2 源区特征

由于岩脉多受到蚀变, 其主量元素特征已受到较大影响, 因此难以利用主量元素组成判别其源区成分演化特征等。而从微量元素特征上看, 除个别元素受到影响外, 其余元素受到蚀变的影响较小。因此可利用微量元素对判断岩脉的源区特征进行识别。岩脉富集大离子亲石元素, 亏损 Ta 和 Nb 等高场强元素, 暗示其源岩可能主要为陆壳沉积物。岩脉的 Nb/Ta 比值为 $2.69 \sim 16.54$ (平均 9.2), 接近于地壳平均值 12.2 , 也暗示岩脉可能主要由地壳物质部分熔融而成 (陈小明等, 2002)。在 Rb/Sr-Rb/Ba 判别图解中 (图 6a), 岩脉样品和周边同期岩体大部分投影于富粘土沉积物区域的

表 3 岩脉的 Hf 同位素特征

Table 3 Hf isotopic compositions of zircons from dykes

| Spot No. | $^{176}\text{Yb}/^{177}\text{Hf}$ | $^{176}\text{Lu}/^{177}\text{Hf}$ | 2 sigma | $^{176}\text{Hf}/^{177}\text{Hf}$ | 2 sigma | Age (Ma) | I_{Hf} | CHUR | DM | $\varepsilon_{\text{Hf}}(t)$ | 2 sigma | $f_{\text{Lu/Hf}}$ | $t_{\text{DM}} (\text{Ma})$ | 2 sigma | $t_{\text{DM}} (\text{Ma})$ | 2 sigma |
|-----------|-----------------------------------|-----------------------------------|----------|-----------------------------------|----------|----------|-----------------|----------|----------|------------------------------|---------|--------------------|-----------------------------|---------|-----------------------------|---------|
| SXC-02-1 | 0.028903 | 0.000849 | 0.000007 | 0.282315 | 0.000021 | 217 | 0.282312 | 0.282637 | 0.283094 | -11.5 | 0.7 | -0.97 | 1318 | 29 | 1973 | 47 |
| SXC-02-2 | 0.031920 | 0.000924 | 0.000009 | 0.282304 | 0.000019 | 217 | 0.282300 | 0.282637 | 0.283094 | -11.9 | 0.7 | -0.97 | 1337 | 27 | 2000 | 42 |
| SXC-02-3 | 0.040977 | 0.001201 | 0.000003 | 0.282329 | 0.000020 | 217 | 0.282324 | 0.282637 | 0.283094 | -11.1 | 0.7 | -0.96 | 1311 | 28 | 1947 | 44 |
| SXC-02-4 | 0.030123 | 0.000902 | 0.000007 | 0.282356 | 0.000021 | 217 | 0.282352 | 0.282637 | 0.283094 | -10.1 | 0.7 | -0.97 | 1263 | 29 | 1884 | 46 |
| SXC-02-5 | 0.028660 | 0.000863 | 0.000004 | 0.282333 | 0.000020 | 217 | 0.282330 | 0.282637 | 0.283094 | -10.9 | 0.7 | -0.97 | 1294 | 28 | 1934 | 45 |
| SXC-02-6 | 0.031678 | 0.000974 | 0.000003 | 0.282288 | 0.000019 | 217 | 0.282284 | 0.282637 | 0.283094 | -12.5 | 0.7 | -0.97 | 1361 | 27 | 2035 | 42 |
| SXC-02-7 | 0.036498 | 0.001128 | 0.000008 | 0.282366 | 0.000019 | 217 | 0.282362 | 0.282637 | 0.283094 | -9.8 | 0.7 | -0.97 | 1256 | 27 | 1863 | 42 |
| SXC-02-8 | 0.023426 | 0.000742 | 0.000008 | 0.282295 | 0.000022 | 217 | 0.282292 | 0.282637 | 0.283094 | -12.2 | 0.8 | -0.98 | 1342 | 30 | 2017 | 48 |
| SXC-02-9 | 0.047689 | 0.001376 | 0.000022 | 0.282448 | 0.000019 | 217 | 0.282442 | 0.282637 | 0.283094 | -6.9 | 0.7 | -0.96 | 1150 | 28 | 1685 | 43 |
| SXC-02-10 | 0.040427 | 0.001129 | 0.000014 | 0.282304 | 0.000018 | 217 | 0.282300 | 0.282637 | 0.283094 | -11.9 | 0.7 | -0.97 | 1343 | 26 | 2000 | 41 |
| SXC-02-11 | 0.032493 | 0.001007 | 0.000005 | 0.282264 | 0.000019 | 217 | 0.282260 | 0.282637 | 0.283094 | -13.4 | 0.7 | -0.97 | 1396 | 26 | 2089 | 41 |
| SXC-02-12 | 0.046422 | 0.001340 | 0.000006 | 0.282409 | 0.000020 | 217 | 0.282404 | 0.282637 | 0.283094 | -8.3 | 0.7 | -0.96 | 1203 | 29 | 1770 | 45 |
| SXC-02-13 | 0.051704 | 0.001398 | 0.000017 | 0.282421 | 0.000023 | 217 | 0.282415 | 0.282637 | 0.283094 | -7.9 | 0.8 | -0.96 | 1188 | 32 | 1744 | 50 |
| SXC-02-14 | 0.040073 | 0.001178 | 0.000005 | 0.282416 | 0.000018 | 217 | 0.282411 | 0.282637 | 0.283094 | -8.0 | 0.6 | -0.96 | 1189 | 25 | 1755 | 40 |
| SXC-02-15 | 0.042471 | 0.001223 | 0.000003 | 0.282443 | 0.000019 | 217 | 0.282408 | 0.282637 | 0.283094 | -8.1 | 0.7 | -0.96 | 1194 | 27 | 1761 | 42 |
| SXC-02-16 | 0.034338 | 0.001029 | 0.000004 | 0.282417 | 0.000019 | 217 | 0.282413 | 0.282637 | 0.283094 | -7.9 | 0.7 | -0.97 | 1182 | 26 | 1750 | 41 |
| SXC-02-17 | 0.044972 | 0.001350 | 0.000005 | 0.282436 | 0.000019 | 217 | 0.282430 | 0.282637 | 0.283094 | -7.3 | 0.7 | -0.96 | 1165 | 27 | 1711 | 43 |
| SXC-02-18 | 0.041835 | 0.001257 | 0.000009 | 0.282376 | 0.000022 | 217 | 0.282371 | 0.282637 | 0.283094 | -9.4 | 0.8 | -0.96 | 1247 | 31 | 1842 | 48 |
| SXC-02-19 | 0.032572 | 0.000988 | 0.000005 | 0.282365 | 0.000019 | 217 | 0.282361 | 0.282637 | 0.283094 | -9.8 | 0.7 | -0.97 | 1253 | 27 | 1864 | 43 |
| SXC-02-20 | 0.034881 | 0.001067 | 0.000008 | 0.282316 | 0.000024 | 217 | 0.282311 | 0.282637 | 0.283094 | -11.5 | 0.8 | -0.97 | 1326 | 33 | 1975 | 52 |
| SXC-02-21 | 0.033489 | 0.001027 | 0.000006 | 0.282305 | 0.000019 | 217 | 0.282301 | 0.282637 | 0.283094 | -11.9 | 0.7 | -0.97 | 1339 | 27 | 1997 | 42 |
| SXC-02-22 | 0.007414 | 0.000256 | 0.000000 | 0.281941 | 0.000020 | 795 | 0.281938 | 0.282276 | 0.282676 | -12.0 | 0.7 | -0.99 | 1809 | 27 | 2438 | 44 |
| SZ-8-1 | 0.038282 | 0.001110 | 0.000006 | 0.282441 | 0.000020 | 220 | 0.282437 | 0.282636 | 0.283092 | -7.0 | 0.7 | -0.97 | 1151 | 28 | 1695 | 44 |
| SZ-8-2 | 0.032130 | 0.000930 | 0.000004 | 0.282366 | 0.000025 | 220 | 0.282362 | 0.282636 | 0.283092 | -9.7 | 0.9 | -0.97 | 1250 | 35 | 1860 | 55 |
| SZ-8-3 | 0.061281 | 0.001619 | 0.000004 | 0.282447 | 0.000020 | 220 | 0.282411 | 0.282636 | 0.283092 | -8.0 | 0.7 | -0.95 | 1200 | 29 | 1753 | 45 |
| SZ-8-4 | 0.036338 | 0.001049 | 0.000007 | 0.282355 | 0.000023 | 220 | 0.282351 | 0.282636 | 0.283092 | -10.1 | 0.8 | -0.97 | 1270 | 33 | 1886 | 52 |
| SZ-8-5 | 0.032298 | 0.000923 | 0.000013 | 0.282412 | 0.000017 | 220 | 0.282408 | 0.282636 | 0.283092 | -8.1 | 0.6 | -0.97 | 1186 | 24 | 1759 | 38 |
| SZ-8-6 | 0.037221 | 0.001094 | 0.000003 | 0.282445 | 0.000023 | 220 | 0.282410 | 0.282636 | 0.283092 | -8.0 | 0.8 | -0.97 | 1187 | 32 | 1753 | 51 |
| SZ-8-7 | 0.042382 | 0.001168 | 0.000001 | 0.282453 | 0.000019 | 220 | 0.282449 | 0.282636 | 0.283092 | -6.6 | 0.7 | -0.96 | 1135 | 26 | 1669 | 41 |
| SZ-8-8 | 0.041352 | 0.001363 | 0.000034 | 0.282434 | 0.000020 | 220 | 0.282429 | 0.282636 | 0.283092 | -7.3 | 0.7 | -0.96 | 1168 | 28 | 1713 | 44 |
| SZ-8-9 | 0.035859 | 0.001043 | 0.000008 | 0.282361 | 0.000017 | 220 | 0.282356 | 0.282636 | 0.283092 | -9.9 | 0.6 | -0.97 | 1262 | 23 | 1873 | 37 |
| SZ-8-10 | 0.042568 | 0.001278 | 0.000003 | 0.282398 | 0.000022 | 220 | 0.282393 | 0.282636 | 0.283092 | -8.6 | 0.8 | -0.96 | 1217 | 31 | 1793 | 49 |
| SZ-8-11 | 0.046625 | 0.001310 | 0.000012 | 0.282380 | 0.000022 | 220 | 0.282375 | 0.282636 | 0.283092 | -9.2 | 0.8 | -0.96 | 1243 | 32 | 1832 | 50 |
| SZ-8-12 | 0.040647 | 0.001171 | 0.000007 | 0.282461 | 0.000026 | 220 | 0.282457 | 0.282636 | 0.283092 | -6.3 | 0.9 | -0.96 | 1124 | 37 | 1651 | 58 |
| SZ-8-13 | 0.039640 | 0.001167 | 0.000008 | 0.282360 | 0.000023 | 220 | 0.282355 | 0.282636 | 0.283092 | -9.9 | 0.8 | -0.96 | 1267 | 33 | 1877 | 52 |
| SZ-8-14 | 0.034042 | 0.001011 | 0.000003 | 0.282383 | 0.000020 | 220 | 0.282379 | 0.282636 | 0.283092 | -9.1 | 0.7 | -0.97 | 1229 | 28 | 1823 | 44 |
| SZ-8-15 | 0.040955 | 0.001225 | 0.000012 | 0.282354 | 0.000020 | 220 | 0.282349 | 0.282636 | 0.283092 | -10.1 | 0.7 | -0.96 | 1277 | 28 | 1889 | 45 |

续表 3
Continued Table 3

| Spot No. | $^{176}\text{Yb}/^{177}\text{Hf}$ | $^{176}\text{Lu}/^{177}\text{Hf}$ | 2 sigma | $^{176}\text{Hf}/^{177}\text{Hf}$ | 2 sigma | Age(Ma) | I_{HF} | CHUR | DM | $\delta_{\text{Hf}}(\text{t})$ | 2 sigma | $f_{\text{Lu/Hf}}$ | $t_{\text{DM}}(\text{Ma})$ | 2 sigma | $t_{\text{DM}}(\text{Ma})$ | 2 sigma |
|----------|-----------------------------------|-----------------------------------|----------|-----------------------------------|----------|---------|-----------------|----------|----------|--------------------------------|---------|--------------------|----------------------------|---------|----------------------------|---------|
| SZ-8-16 | 0.031494 | 0.000962 | 0.000004 | 0.282415 | 0.000018 | 220 | 0.282411 | 0.282636 | 0.283092 | -7.9 | 0.6 | -0.97 | 1182 | 25 | 1751 | 40 |
| SZ-8-17 | 0.035265 | 0.001036 | 0.000011 | 0.282384 | 0.000022 | 220 | 0.282380 | 0.282636 | 0.283092 | -9.0 | 0.8 | -0.97 | 1228 | 31 | 1821 | 48 |
| SZ-8-18 | 0.033407 | 0.000995 | 0.000005 | 0.282456 | 0.000019 | 220 | 0.282452 | 0.282636 | 0.283092 | -6.5 | 0.7 | -0.97 | 1126 | 27 | 1661 | 43 |
| SZ-8-19 | 0.030405 | 0.000899 | 0.000015 | 0.282494 | 0.000020 | 220 | 0.282491 | 0.282636 | 0.283092 | -5.1 | 0.7 | -0.97 | 1070 | 29 | 1576 | 45 |
| SZ-8-20 | 0.039702 | 0.001167 | 0.000004 | 0.282294 | 0.000020 | 220 | 0.282289 | 0.282636 | 0.283092 | -12.3 | 0.7 | -0.96 | 1360 | 28 | 2022 | 44 |
| SZ-8-21 | 0.030548 | 0.000895 | 0.000002 | 0.282328 | 0.000018 | 220 | 0.282324 | 0.282636 | 0.283092 | -11.0 | 0.6 | -0.97 | 1302 | 25 | 1944 | 39 |
| ZW-01-1 | 0.026674 | 0.000805 | 0.000005 | 0.282449 | 0.000020 | 217 | 0.282416 | 0.282637 | 0.283094 | -7.8 | 0.7 | -0.98 | 1172 | 27 | 1744 | 43 |
| ZW-01-2 | 0.031197 | 0.000951 | 0.000004 | 0.282352 | 0.000018 | 217 | 0.282348 | 0.282637 | 0.283094 | -10.2 | 0.7 | -0.97 | 1270 | 26 | 1893 | 41 |
| ZW-01-3 | 0.036210 | 0.001084 | 0.000001 | 0.282365 | 0.000022 | 217 | 0.282360 | 0.282637 | 0.283094 | -9.8 | 0.8 | -0.97 | 1257 | 31 | 1867 | 49 |
| ZW-01-4 | 0.036935 | 0.000929 | 0.000006 | 0.282487 | 0.000018 | 217 | 0.282483 | 0.282637 | 0.283094 | -5.5 | 0.6 | -0.97 | 1081 | 25 | 1595 | 40 |
| ZW-01-5 | 0.038379 | 0.001154 | 0.000010 | 0.282494 | 0.000020 | 217 | 0.282490 | 0.282637 | 0.283094 | -5.2 | 0.7 | -0.97 | 1077 | 28 | 1580 | 44 |
| ZW-01-6 | 0.035770 | 0.001089 | 0.000007 | 0.282443 | 0.000020 | 217 | 0.282439 | 0.282637 | 0.283094 | -7.0 | 0.7 | -0.97 | 1147 | 28 | 1693 | 44 |
| ZW-01-7 | 0.025136 | 0.000789 | 0.000004 | 0.282134 | 0.000016 | 728 | 0.282123 | 0.282318 | 0.282725 | -6.9 | 0.6 | -0.98 | 1568 | 23 | 2072 | 36 |
| ZW-01-8 | 0.029391 | 0.000904 | 0.000015 | 0.282385 | 0.000018 | 217 | 0.282382 | 0.282637 | 0.283094 | -9.0 | 0.6 | -0.97 | 1222 | 26 | 1819 | 41 |
| ZW-01-9 | 0.030657 | 0.000932 | 0.000001 | 0.282432 | 0.000017 | 217 | 0.282428 | 0.282637 | 0.283094 | -7.4 | 0.6 | -0.97 | 1158 | 24 | 1716 | 38 |
| ZW-01-10 | 0.033558 | 0.001046 | 0.000007 | 0.282441 | 0.000022 | 217 | 0.282437 | 0.282637 | 0.283094 | -7.1 | 0.8 | -0.97 | 1148 | 31 | 1696 | 50 |
| ZW-01-11 | 0.036066 | 0.001135 | 0.000005 | 0.282394 | 0.000020 | 217 | 0.282389 | 0.282637 | 0.283094 | -8.8 | 0.7 | -0.97 | 1218 | 29 | 1803 | 45 |
| ZW-01-12 | 0.044211 | 0.001219 | 0.000005 | 0.282293 | 0.000020 | 217 | 0.282288 | 0.282637 | 0.283094 | -12.4 | 0.7 | -0.96 | 1363 | 28 | 2026 | 45 |
| ZW-01-13 | 0.008412 | 0.000292 | 0.000000 | 0.281982 | 0.000021 | 627 | 0.281979 | 0.282381 | 0.282798 | -14.3 | 0.7 | -0.99 | 1755 | 28 | 2451 | 45 |
| ZW-01-14 | 0.050111 | 0.001411 | 0.000005 | 0.282439 | 0.000019 | 217 | 0.282433 | 0.282637 | 0.283094 | -7.2 | 0.7 | -0.96 | 1164 | 26 | 1706 | 41 |
| ZW-01-15 | 0.027199 | 0.000808 | 0.000005 | 0.282357 | 0.000022 | 217 | 0.282353 | 0.282637 | 0.283094 | -10.1 | 0.8 | -0.98 | 1259 | 31 | 1882 | 49 |
| ZW-01-16 | 0.034469 | 0.001006 | 0.000002 | 0.282427 | 0.000020 | 217 | 0.282423 | 0.282637 | 0.283094 | -7.6 | 0.7 | -0.97 | 1168 | 28 | 1729 | 44 |
| ZW-01-17 | 0.037627 | 0.001123 | 0.000003 | 0.282437 | 0.000020 | 217 | 0.282433 | 0.282637 | 0.283094 | -7.2 | 0.7 | -0.97 | 1157 | 28 | 1706 | 43 |
| ZW-01-18 | 0.038567 | 0.001150 | 0.000005 | 0.282420 | 0.000018 | 217 | 0.282416 | 0.282637 | 0.283094 | -7.8 | 0.6 | -0.97 | 1181 | 26 | 1744 | 40 |
| ZW-01-19 | 0.041725 | 0.001226 | 0.000003 | 0.282356 | 0.000019 | 217 | 0.282351 | 0.282637 | 0.283094 | -10.1 | 0.7 | -0.96 | 1274 | 27 | 1887 | 43 |
| ZW-01-20 | 0.031268 | 0.000976 | 0.000008 | 0.282392 | 0.000019 | 217 | 0.282388 | 0.282637 | 0.283094 | -8.8 | 0.7 | -0.97 | 1216 | 26 | 1806 | 41 |
| ZW-01-21 | 0.056225 | 0.001604 | 0.000001 | 0.282465 | 0.000018 | 217 | 0.282459 | 0.282637 | 0.283094 | -6.3 | 0.6 | -0.95 | 1131 | 26 | 1648 | 40 |
| ZW-01-22 | 0.038958 | 0.001156 | 0.000004 | 0.282379 | 0.000019 | 217 | 0.282374 | 0.282637 | 0.283094 | -9.3 | 0.7 | -0.97 | 1240 | 26 | 1836 | 42 |
| FC-05-01 | 0.029630 | 0.000879 | 0.000014 | 0.282383 | 0.000017 | 220 | 0.282379 | 0.282636 | 0.283092 | -9.1 | 0.6 | -0.97 | 1225 | 24 | 1822 | 38 |
| FC-05-02 | 0.038275 | 0.001185 | 0.000003 | 0.282379 | 0.000020 | 220 | 0.282375 | 0.282636 | 0.283092 | -9.2 | 0.7 | -0.96 | 1240 | 28 | 1833 | 44 |
| FC-05-03 | 0.035229 | 0.001057 | 0.000001 | 0.282451 | 0.000019 | 220 | 0.282447 | 0.282636 | 0.283092 | -6.7 | 0.7 | -0.97 | 1134 | 27 | 1672 | 43 |
| FC-05-04 | 0.045654 | 0.001347 | 0.000018 | 0.282449 | 0.000021 | 220 | 0.282443 | 0.282636 | 0.283092 | -6.8 | 0.7 | -0.96 | 1147 | 29 | 1681 | 46 |
| FC-05-05 | 0.055350 | 0.001197 | 0.000018 | 0.282474 | 0.000027 | 220 | 0.282467 | 0.282636 | 0.283092 | -6.0 | 1.0 | -0.95 | 1124 | 39 | 1628 | 61 |
| FC-05-06 | 0.062115 | 0.001812 | 0.000023 | 0.282531 | 0.000023 | 220 | 0.282523 | 0.282636 | 0.283092 | -4.0 | 0.8 | -0.95 | 1044 | 33 | 1503 | 50 |
| FC-05-07 | 0.039306 | 0.001155 | 0.000009 | 0.282479 | 0.000016 | 220 | 0.282475 | 0.282636 | 0.283092 | -5.7 | 0.6 | -0.97 | 1098 | 22 | 1611 | 35 |
| FC-05-08 | 0.032781 | 0.000976 | 0.000007 | 0.282280 | 0.000020 | 220 | 0.282276 | 0.282636 | 0.283092 | -12.7 | 0.7 | -0.97 | 1372 | 29 | 2051 | 45 |

续表 3
Continued Table 3

| Spot No. | $^{176}\text{Yb}/^{177}\text{Hf}$ | $^{176}\text{Lu}/^{177}\text{Hf}$ | 2 sigma | $^{176}\text{Hf}/^{177}\text{Hf}$ | 2 sigma | Age (Ma) | I_{hf} | CHUR | DM | $\varepsilon_{\text{Hf}}(t)$ | 2 sigma | $f_{\text{Lu/Hf}}$ | $t_{\text{DM1}}(\text{Ma})$ | 2 sigma | $t_{\text{DM2}}(\text{Ma})$ | 2 sigma |
|-----------|-----------------------------------|-----------------------------------|----------|-----------------------------------|----------|----------|-----------------|----------|----------|------------------------------|---------|--------------------|-----------------------------|---------|-----------------------------|---------|
| FC-05-09 | 0.031006 | 0.000933 | 0.000001 | 0.282411 | 0.000019 | 220 | 0.282407 | 0.282636 | 0.283092 | -8.1 | 0.7 | -0.97 | 1188 | 26 | 1761 | 41 |
| FC-05-10 | 0.057609 | 0.001616 | 0.000012 | 0.282432 | 0.000016 | 220 | 0.282425 | 0.282636 | 0.283092 | -7.4 | 0.6 | -0.95 | 1180 | 23 | 1721 | 35 |
| FC-05-11 | 0.038127 | 0.001135 | 0.000013 | 0.282354 | 0.000023 | 220 | 0.282349 | 0.282636 | 0.283092 | -10.1 | 0.8 | -0.97 | 1274 | 32 | 1889 | 50 |
| FC-05-12 | 0.057505 | 0.001603 | 0.000016 | 0.282402 | 0.000016 | 220 | 0.282395 | 0.282636 | 0.283092 | -8.5 | 0.6 | -0.95 | 1222 | 22 | 1787 | 35 |
| FC-05-13 | 0.046351 | 0.001296 | 0.000016 | 0.282416 | 0.000018 | 220 | 0.282410 | 0.282636 | 0.283092 | -8.0 | 0.6 | -0.96 | 1192 | 26 | 1753 | 40 |
| FC-05-14 | 0.038002 | 0.001264 | 0.000017 | 0.282476 | 0.000020 | 220 | 0.282471 | 0.282636 | 0.283092 | -5.8 | 0.7 | -0.96 | 1106 | 28 | 1619 | 44 |
| FC-05-15 | 0.046341 | 0.001567 | 0.000054 | 0.282369 | 0.000022 | 220 | 0.282302 | 0.282636 | 0.283092 | -11.8 | 0.8 | -0.95 | 1353 | 31 | 1993 | 48 |
| FC-05-16 | 0.042587 | 0.001339 | 0.000020 | 0.282285 | 0.000019 | 220 | 0.282279 | 0.282636 | 0.283092 | -12.6 | 0.7 | -0.96 | 1379 | 26 | 2044 | 41 |
| FC-05-17 | 0.049287 | 0.001483 | 0.000012 | 0.282389 | 0.000017 | 220 | 0.282383 | 0.282636 | 0.283092 | -8.9 | 0.6 | -0.96 | 1236 | 24 | 1814 | 37 |
| FC-05-18 | 0.078905 | 0.002428 | 0.000050 | 0.282380 | 0.000021 | 220 | 0.282370 | 0.282636 | 0.283092 | -9.4 | 0.7 | -0.93 | 1281 | 30 | 1842 | 46 |
| FC-05-19 | 0.040465 | 0.001304 | 0.000032 | 0.282348 | 0.000019 | 220 | 0.282343 | 0.282636 | 0.283092 | -10.3 | 0.7 | -0.96 | 1288 | 26 | 1903 | 41 |
| FC-05-20 | 0.060886 | 0.001991 | 0.000025 | 0.282341 | 0.000038 | 220 | 0.282333 | 0.282636 | 0.283092 | -10.7 | 1.4 | -0.94 | 1323 | 55 | 1926 | 85 |
| WTC-10-01 | 0.031332 | 0.000901 | 0.000009 | 0.282363 | 0.000022 | 218 | 0.282359 | 0.282637 | 0.283094 | -9.8 | 0.8 | -0.97 | 1254 | 31 | 1868 | 49 |
| WTC-10-02 | 0.024926 | 0.000790 | 0.000006 | 0.282496 | 0.000021 | 218 | 0.282493 | 0.282637 | 0.283094 | -5.1 | 0.7 | -0.98 | 1064 | 29 | 1571 | 47 |
| WTC-10-03 | 0.028164 | 0.000869 | 0.000011 | 0.282490 | 0.000018 | 218 | 0.282486 | 0.282637 | 0.283094 | -5.3 | 0.6 | -0.97 | 1075 | 25 | 1586 | 39 |
| WTC-10-04 | 0.007468 | 0.000253 | 0.000000 | 0.282026 | 0.000019 | 777 | 0.282023 | 0.282287 | 0.282689 | -9.4 | 0.7 | -0.99 | 1693 | 26 | 2262 | 42 |
| WTC-10-05 | 0.036427 | 0.001167 | 0.000003 | 0.282445 | 0.000023 | 218 | 0.282440 | 0.282637 | 0.283094 | -7.0 | 0.8 | -0.96 | 1148 | 32 | 1690 | 50 |
| WTC-10-06 | 0.026474 | 0.000897 | 0.000003 | 0.282437 | 0.000021 | 218 | 0.282434 | 0.282637 | 0.283094 | -7.2 | 0.7 | -0.97 | 1149 | 29 | 1703 | 46 |
| WTC-10-07 | 0.023093 | 0.000745 | 0.000001 | 0.282536 | 0.000017 | 218 | 0.282533 | 0.282637 | 0.283094 | -3.7 | 0.6 | -0.98 | 1007 | 24 | 1482 | 39 |
| WTC-10-08 | 0.021396 | 0.000698 | 0.000003 | 0.282471 | 0.000020 | 218 | 0.282468 | 0.282637 | 0.283094 | -6.0 | 0.7 | -0.98 | 1096 | 27 | 1626 | 44 |
| WTC-10-09 | 0.031677 | 0.000935 | 0.000009 | 0.282457 | 0.000020 | 218 | 0.282454 | 0.282637 | 0.283094 | -6.5 | 0.7 | -0.97 | 1122 | 28 | 1659 | 44 |
| WTC-10-10 | 0.036518 | 0.001131 | 0.000016 | 0.282481 | 0.000021 | 218 | 0.282476 | 0.282637 | 0.283094 | -5.7 | 0.7 | -0.97 | 1095 | 29 | 1608 | 46 |
| WTC-10-11 | 0.022144 | 0.000748 | 0.000006 | 0.282499 | 0.000022 | 218 | 0.282496 | 0.282637 | 0.283094 | -5.0 | 0.8 | -0.98 | 1059 | 31 | 1566 | 50 |
| WTC-10-12 | 0.039120 | 0.001267 | 0.000003 | 0.282457 | 0.000018 | 218 | 0.282452 | 0.282637 | 0.283094 | -6.5 | 0.6 | -0.96 | 1133 | 26 | 1663 | 40 |
| WTC-10-13 | 0.007897 | 0.000258 | 0.000000 | 0.281990 | 0.000019 | 738 | 0.281987 | 0.282312 | 0.282718 | -11.5 | 0.7 | -0.99 | 1742 | 26 | 2365 | 42 |
| WTC-10-14 | 0.057761 | 0.001631 | 0.000030 | 0.282492 | 0.000019 | 218 | 0.282485 | 0.282637 | 0.283094 | -5.4 | 0.7 | -0.95 | 1094 | 26 | 1589 | 41 |
| WTC-10-15 | 0.036230 | 0.001124 | 0.000008 | 0.282379 | 0.000017 | 218 | 0.282375 | 0.282637 | 0.283094 | -9.3 | 0.6 | -0.97 | 1238 | 23 | 1834 | 37 |
| WTC-10-16 | 0.035700 | 0.001123 | 0.000005 | 0.282445 | 0.000020 | 218 | 0.282441 | 0.282637 | 0.283094 | -6.9 | 0.7 | -0.97 | 1145 | 28 | 1687 | 44 |
| WTC-10-17 | 0.031480 | 0.001013 | 0.000010 | 0.282446 | 0.000020 | 218 | 0.282412 | 0.282637 | 0.283094 | -7.9 | 0.7 | -0.97 | 1183 | 28 | 1751 | 44 |
| WTC-10-18 | 0.030039 | 0.000896 | 0.000004 | 0.282398 | 0.000020 | 218 | 0.282395 | 0.282637 | 0.283094 | -8.6 | 0.7 | -0.97 | 1204 | 28 | 1790 | 44 |
| WTC-10-19 | 0.066017 | 0.001799 | 0.000015 | 0.282448 | 0.000019 | 218 | 0.282441 | 0.282637 | 0.283094 | -6.9 | 0.7 | -0.95 | 1162 | 28 | 1687 | 43 |
| WTC-10-20 | 0.035049 | 0.001150 | 0.000005 | 0.282470 | 0.000019 | 218 | 0.282466 | 0.282637 | 0.283094 | -6.1 | 0.7 | -0.97 | 1111 | 27 | 1632 | 42 |
| WTC-10-21 | 0.045900 | 0.001292 | 0.000011 | 0.282443 | 0.000017 | 218 | 0.282408 | 0.282637 | 0.283094 | -8.1 | 0.6 | -0.96 | 1196 | 24 | 1761 | 37 |
| WTC-10-22 | 0.036283 | 0.001134 | 0.000002 | 0.282466 | 0.000021 | 218 | 0.282462 | 0.282637 | 0.283094 | -6.2 | 0.7 | -0.97 | 1116 | 29 | 1641 | 46 |
| WTC-10-23 | 0.055016 | 0.0011581 | 0.000016 | 0.282434 | 0.000019 | 218 | 0.282428 | 0.282637 | 0.283094 | -7.4 | 0.7 | -0.95 | 1175 | 27 | 1717 | 42 |
| WTC-10-24 | 0.032282 | 0.001050 | 0.000009 | 0.282417 | 0.000016 | 218 | 0.282413 | 0.282637 | 0.283094 | -7.9 | 0.6 | -0.97 | 1182 | 22 | 1749 | 35 |
| WTC-10-25 | 0.063820 | 0.001715 | 0.000019 | 0.282474 | 0.000017 | 218 | 0.282467 | 0.282637 | 0.283094 | -6.0 | 0.6 | -0.95 | 1122 | 24 | 1629 | 37 |

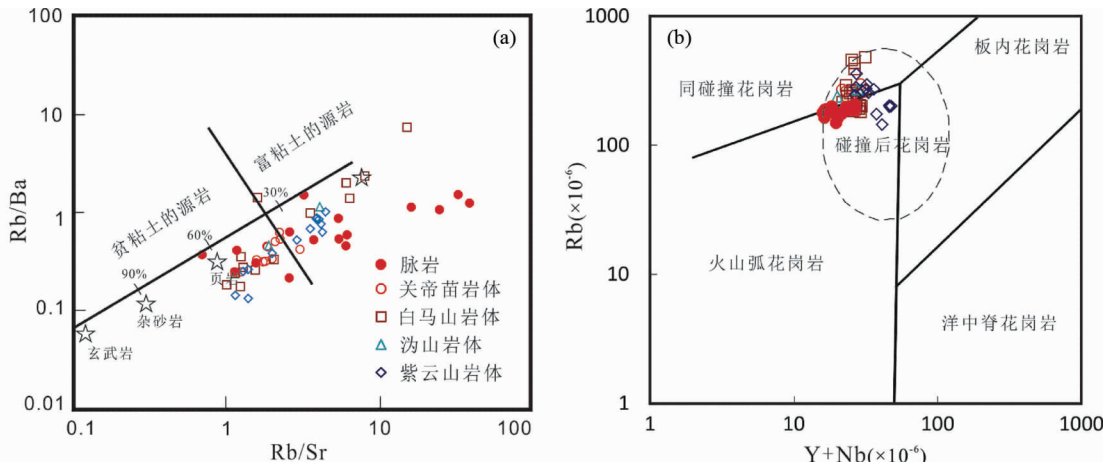


图6 岩脉的 Rb/Sr-Rb/Ba 图解(a, 据 Sylvester, 1998) 和 Rb-Y + Nb 图解(b, 据 Pearce *et al.*, 1984)

Fig. 6 Rb/Sr vs. Rb/Ba diagram (a, after Sylvester, 1998) and Rb vs. Y + Nb diagram (b, after Pearce *et al.*, 1984) of dykes

泥质岩熔体附近,表明岩脉与周边印支期晚期大岩体的源区相似,主要由大陆地壳的富粘土的泥质岩石部分熔融而成。研究表明,锆石的微量元素组成受控于岩浆演化,利用锆石中的微量元素之间的相关性,也可以对岩浆起源及成分演化等进行识别(Hoskin and Schaltegger, 2003; Grimes *et al.*, 2007; Wang *et al.*, 2012)。在锆石的 U/Yb-Hf 和 U/Yb-Y 图解中(图 7a, b),酸性岩脉的大部分样品均位于大陆锆石内,暗示这些岩脉主要来源于壳源物质。在锆石的 Th-Pb 和 $(Nb/Pb)_N-Eu/Eu^*$ 图解中(图 7c, d),酸性岩脉的样品几乎都投影于 S 型花岗岩类锆石区域,表明所测定锆石具有 S 型花岗岩类锆石的特征,而且这些锆石均具有明显的负 Eu 异常,显示岩脉具有 S 型花岗岩的特征,可以主要来源于壳源物质的部分熔融。

锆石的 Hf 同位素结果显示,花岗岩脉的 $\varepsilon_{Hf}(t)$ 均为负值($-13.4 \sim -3.7$)(图 8a),在 $\varepsilon_{Hf}(t)$ -Age 图解上所有样品点均落在亏损地幔及球粒陨石演化线之下(图 8b),暗示其为古老地壳部分熔融的产物,同时而其古老的二阶模式年龄 t_{DM2} 为 2089 ~ 1482 Ma 表明,酸性岩脉群来源于早元古代-中元古代变质沉积岩部分熔融。获得的几颗捕获锆石具有一致的新元古代年龄和亏损的 Hf 同位素特征,暗示岩脉的源区其形成过程中可能有少量新元古代壳源物质加入。

4.3 构造意义

近年来学者对华南地区印支期花岗岩开展了大量的高精度年代学研究,其结果显示印支期花岗岩的形成年龄主要集中在两个区间:印支早期(243 ~ 228 Ma)和印支晚期(220 ~ 206)(王岳军等, 2005; 孙涛, 2006; Wang *et al.*, 2007, 2013; 于津海等, 2007; Mao *et al.*, 2013),这些花岗岩的成岩年龄均明显滞后于印支运动变质作用的峰期(258 ~ 243 Ma; Carter *et al.*, 2001)。尽管对于挤压-伸展的转换具体时间还存在着一定的争议(孙涛, 2006; Zhou *et al.*,

2006; Wang *et al.*, 2007; 于津海等, 2007; Fu *et al.*, 2015),但一般认为华南陆块印支早期的花岗岩的形成于可能与印支运动造成的同碰撞挤压构造有关,而印支晚期的花岗岩可能印支运动后碰撞伸展构造机制有关(Zhou *et al.*, 2006; 于津海等, 2007; Wang *et al.*, 2007; Zhao *et al.*, 2013; 廉建仁等, 2014)。

本次研究表明,龙山地区酸性岩脉的成岩年龄为 220 ~ 217 Ma,时间上滞后于印支运动造山运动高峰期约 20 ~ 30 Ma。地球化学特征显示岩脉及其周边花岗岩均是在碰撞后的伸展环间中形成(图 6b),表明此时湘中地区受控于碰撞后的岩石圈伸展的构造机制,华南陆块整体已进入后碰撞的应力松弛阶段。正是在这种伸展构造背景下,基底古元古代-中元古代变质泥岩受到减压作用,部分熔融并向上侵位,形成了龙山地区酸性岩脉及周边大规模印支晚期花岗岩体。

4.4 成矿意义

由于湘中地区低温金锑矿床空间上与岩浆岩体的关系不明显,同时周边出露的大花岗岩体为印支期岩体(丁兴等, 2005, 2012; 王岳军等, 2005; 李建华等, 2014; 刘凯等, 2014; Fu *et al.*, 2015; 赵增霞等, 2015),而前人成矿年代学研究显示湘中地区的金锑低温矿床主要时代为加里东晚期和燕山早期(罗纲元, 1994; 史明魁等, 1994; 彭建堂和胡瑞忠, 2001; 吴良士和胡雄伟, 2000; Peng *et al.*, 2003),因此许多学者认为岩浆活动与金锑成矿之间并无联系。但越来越多的证据表明湘中地区发育印支晚期金锑矿化(肖启明等, 1992; 姚振凯和朱蓉斌, 1993; 彭渤和陈广浩, 2000; Peng and Frei, 2004; 孙际茂等, 2007; 李华芹等, 2008; 陈新跃等, 2012; 付山岭等, 2016),并且一些与金锑矿床密切相关的酸性岩脉的成龄年龄被证明为印支晚期(肖启明等, 1992; 姚振凯和朱蓉斌, 1993; 赵军红等, 2005)。如廖家坪和符竹溪金矿中含矿花岗斑岩的成岩年龄分别为 200 Ma

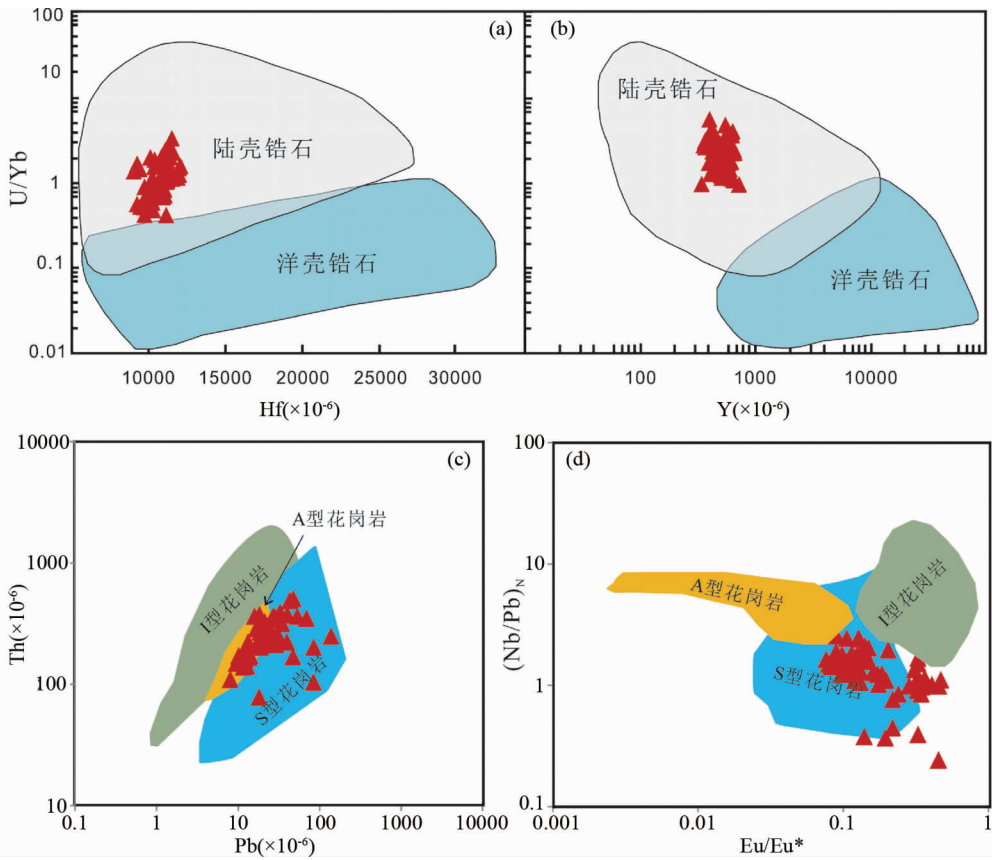


图 7 岩脉中锆石的 U/Yb-Hf 图解 (a)、U/Yb-Y 图解 (b) (a,b, 据 Grimes *et al.*, 2007) 和 Th-Pb 图解 (c)、(Nb/Pb)_N-Eu/Eu^{*} 图解 (d) (c,d, 据 Wang *et al.*, 2012)

Fig. 7 U/Yb vs. Hf diagram (a), U/Yb vs. Y diagram (b) (a, b, after Grimes *et al.*, 2007)) and Th vs. Pb diagram (a), (Nb/Pb)_N vs. Eu/Eu^{*} (c, d, after Wang *et al.*, 2012) of zircons from dykes

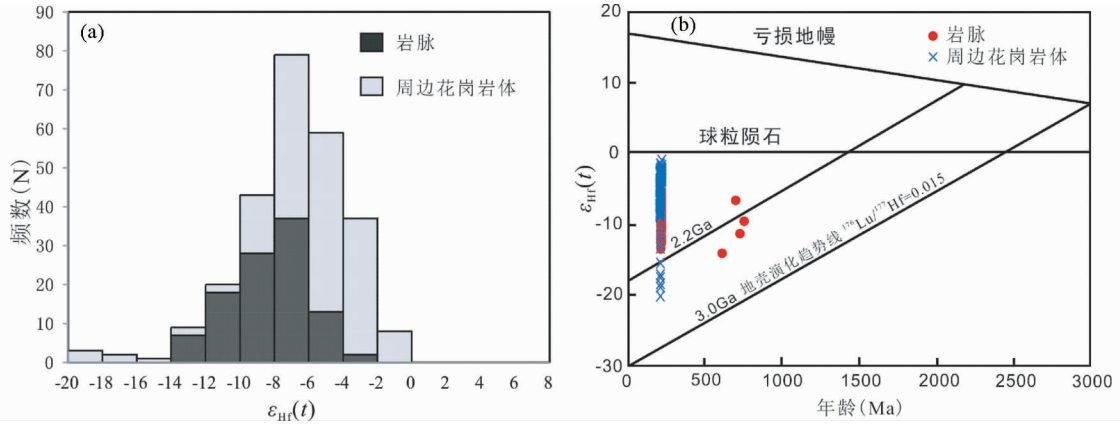


图 8 岩脉及周边花岗岩体的 Hf 同位素组成特征 (a) 和 $\varepsilon_{\text{Hf}}(t)$ -Age 图解 (b)

周边花岗岩体为白马山岩体、沩山岩体和紫云山岩体, 数据据 Fu *et al.*, 2015

Fig. 8 Zircon Hf isotopic compositions (a) and $\varepsilon_{\text{Hf}}(t)$ -Age diagram (b) of the dyke and plutons nearby

Data of Baimashan, Weishan and Ziyuanshan plutons from Fu *et al.*, 2015

(肖启明等, 1992) 和 209 Ma (姚振凯和朱蓉斌, 1993); 而李华芹等(2008)对铲子坪和大坪金矿开展的含金石英脉流体包裹体 Rb-Sr 等时线年龄为 204 Ma 和 205 Ma, 其相关的黄茅

园黑云母花岗岩的 SHRIMP 年龄为 222 Ma, 提出该矿床应为岩浆热液型, 成矿作用可能与酸性岩浆侵位密切相关。以上研究表明, 湘中地区一些金锑成矿与岩浆活动在时间和空间

上均较为吻合,暗示印支晚期岩浆活动与湘中地区金锑矿化有着密切的关系。

由于缺少适合传统放射性同位素定年的矿物,前人对龙山金锑矿的成矿年龄研究较少,开展的流体包裹体 Rb-Sr 法成矿年龄为 175 ± 27 Ma(史明魁等, 1994),暗示龙山金锑成矿发生在印支晚期至燕山早期期间。而梁华英(1989)通过辉锑矿同位素的差异,将龙山金锑矿床成矿作用分为两期。吴运军(2003)通过对矿区成矿构造分析结果表明,龙山金锑矿的容矿构造空间,提出龙山矿床的成矿作用应发生在印支晚期至燕山早期,并且认为印支晚期矿化的成矿流体为岩浆流体。吴继承等(2007)年通过流体包裹体的对比研究,认为龙山金锑矿经历了多期次成矿作用,且成矿流体以岩浆流体为主。庞保成等(2011)通过对龙山矿床中黄铁矿的微量元素研究提出,龙山金锑矿至少经历了两个成矿期,并认为早期矿化是由深部岩浆流体引发。上述研究均暗示龙山金锑矿可能在印支晚期存在一次矿化。这也与我们近期在龙山金锑矿获得的印支晚期成矿年龄相吻合(付山岭等, 2016)。本次研究获得龙山金锑矿外围出露酸性岩脉的具有较为一致的成岩年龄为 $220 \sim 217$ Ma,其成岩时间与龙山金锑矿印支晚期的成矿年龄相吻合。

前人对龙山金锑矿开展的流体包裹体稳定同位素结果显示,龙山金锑矿的成矿流体可能是大气降水与岩浆水的混合(马东升等, 2003; 吴继承等, 2007; 唐朝晖, 2012)。硫化物的硫同位素也显示成矿流体中主要为岩浆硫(马东升等, 2003; 刘鹏程等, 2008),表明成矿流体中具有岩浆流体成分,暗示岩浆活动可能为龙山金锑矿床提供成矿流体来源。另一方面前人的区域地层地球化学研究、铅同位素和淋滤实验均表明(梁华英, 1989; 彭渤和陈广浩, 2000; 马东升等, 2002, 2003),矿区围岩及基底的前寒武系地层具有较高的 Au、Sb 含量及浸出率,可能是龙山金锑矿床的 Sb、Au 成矿元素主要的来源。而酸性脉岩的地球化学研究表明,岩脉具有相对较低的成矿元素含量,暗示岩浆活动不能提供足够的成矿元素,可能不是成矿元素的主要来源。结合年代学的证据,我们认为印支晚期的岩浆活动对龙山金锑矿可能是龙山金锑矿成矿的重要的热源和流体来源之一。

5 结论

(1)酸性岩脉的锆石的 LA-ICP-MS U-Pb 定年显示,龙山金锑矿外围发育的酸性岩脉主要形成于印支晚期($220 \sim 217$ Ma)。

(2)酸性岩脉的元素地球化学和锆石的 Hf 同位素显示,酸性岩脉主要来源于印支运动碰撞后伸展背景下,古元古代-中元古代变质沉积岩减压部分熔融。

(3)印支晚期岩浆活动可能为龙山金锑矿床的成矿事件提供了重要的热源和流体来源之一。

致谢 野外地质采样得到湖南娄底 418 地质队贺文华院长和龙山矿床的周靖平主任的大力帮助;实验分析过程中得到中国科学院地球化学研究所戴智慧高级工程师以及天津地调中心耿建成老师的帮助;北京地质科学院的张志远博士帮忙描绘了部分图件;还得到了两位评审人的建设性评述和宝贵的修改意见;在此谨致谢意。

References

- Amelin Y, Lee DC, Halliday AN and Pidgeon RT. 1999. Nature of the Earth's earliest crust from hafnium isotopes in single detrital zircons. *Nature*, 399(6733): 252–255
- Bai DY, Zhong X, Jia PY, Xiong X and Huang WY. 2014. Geochemistry and petrogenesis of the Indosinian Guandimiao granitic pluton in central Hunan. *Sedimentary Geology and Tethyan Geology*, 34(4): 92–104 (in Chinese with English abstract)
- Bao X and Chen F. 1995. Regional geology of Hunan Province. *Hunan Metallurgy*, (6): 24–28, 46 (in Chinese)
- Bao X, Wan RJ and Bao JM. 2000. Geological features and prospecting criteria of Pre-Cambrian antimony-arsenic-gold deposit in central Hunan. *Hunan Metallurgy*, (5): 34–39 (in Chinese with English abstract)
- Bao ZX, Wan RJ and Bao JM. 2002. Relationship between felsic dikes in Precambrian system strata and gold mineralization in Hunan. *Gold Geology*, 8(1): 33–39 (in Chinese with English abstract)
- Belousova E, Griffin WL, O'reilly SY and Fisher NL. 2002. Igneous zircon: Trace element composition as an indicator of source rock type. *Contributions to Mineralogy and Petrology*, 143(5): 602–622
- Blichert-Toft J and Albarède F. 1997. The Lu-Hf isotope geochemistry of chondrites and the evolution of the mantle-crust system. *Earth and Planetary Science Letters*, 148(1–2): 243–258
- Bureau of Geology and Mineral Resources of Hunan Province. 1988. *Regional Geology of Hunan Province*. Beijing: Geological Publishing House, 1–467 (in Chinese)
- Carter A, Roques D, Bristow C and Kinny P. 2001. Understanding Mesozoic accretion in Southeast Asia: Significance of Triassic thermotectonism (Indosinian orogeny) in Vietnam. *Geology*, 29(3): 211–214
- Chen WF, Chen PR, Huang HY, Ding X and Sun T. 2007. Chronological and geochemical studies of granite and enclave in Baimashan pluton, Hunan, South China. *Science in China (Series D)*, 50(11): 1606–1627
- Chen XM, Wang RC, Liu CS, Hu H, Zhang WL and Gao JF. 2002. Isotopic dating and genesis for Fogang biotite granites of Conghua area, Guangdong Province. *Geological Journal of China Universities*, 8(3): 293–307 (in Chinese with English abstract)
- Chen XY, Yin P, Kuang WL, Dai DQ and Zi F. 2012. Advance research of Au multi-metal metallogenic belt in Xuefeng region, western Hunan Province. *Geological Science and Technology Information*, 31(3): 82–88 (in Chinese with English abstract)
- Compston W, Williams IS, Kirschvink JL, Zhang ZC and Ma GG. 1992. Zircon U-Pb ages for the Early Cambrian time-scale. *Journal of the Geological Society*, 149(2): 171–184
- Corfu F, Hanchar JM, Hoskin PWO and Kinny P. 2003. Atlas of zircon textures. *Reviews in Mineralogy and Geochemistry*, 53(1): 469–500
- Ding X, Chen PR, Chen WF, Huang HY and Zhou XM. 2006. Single zircon LA-ICPMS U-Pb dating of Weishan granite (Hunan, South China) and its petrogenetic significance. *Science in China (Series D)*, 49(8): 816–827
- Ding X, Sun WD, Wang FY, Chen LL, Li QL and Chen FK. 2012. Single-grain mica Rb-Sr isochron ages and mineral chemistry for the

- Weishan pluton in Hunan Province and implications on petrogenesis and mineralization of Mesozoic composite granite in South China. *Acta Petrologica Sinica*, 28 (12) : 3823 – 3840 (in Chinese with English abstract)
- Fu SL, Hu RZ, Bi XW, Chen YW, Yang JH and Huang Y. 2015. Origin of Triassic granites in central Hunan Province, South China: Constraints from zircon U-Pb ages and Hf and O isotopes. *International Geology Review*, 57(2) : 97 – 111
- Fu SL, Hu RZ, Chen YW and Luo JC. 2016. Chronology of the Longshan Au-Sb deposit in central Hunan Province: Constraints from pyrite Re-Os and zircon U-Th/He isotopic dating. *Acta Petrologica Sinica*, 32(11) : 3507 – 3517 (in Chinese with English abstract)
- Grimes CB, John BE, Kelemen PB, Mazdab FK, Wooden JL, Cheadle MJ, Hanghøj K and Schwartz JJ. 2007. Trace element chemistry of zircons from oceanic crust: A method for distinguishing detrital zircon provenance. *Geology*, 35(7) : 643 – 646
- Guan JL, Geng QR, Wang GZ, Peng ZM, Zhang Z, Kou FD, Cong F and Li N. 2014. Geochemical, zircon U-Pb dating and Hf isotope compositions studies of the granite in Ritu County-Lameila Pass area, North Gangdse, Tibet. *Acta Petrologica Sinica*, 30(6) : 1666 – 1684 (in Chinese with English abstract)
- Hanchar JM and van Westrenen W. 2007. Rare earth element behavior in zircon-melt systems. *Elements*, 3(1) : 37 – 42
- He WH, Kang RH, Liu DY, Ma WL, Xie BW and Hu XY. 2015. The ore-controlling structure regularities and prospecting direction in Longshan Au-Sb deposit, Hunan Province. *Geology and Mineral Resources of South China*, 31(3) : 261 – 267 (in Chinese with English abstract)
- Hoskin PWO and Black LP. 2000. Metamorphic zircon formation by solid-state recrystallization of protolith igneous zircon. *Journal of Metamorphic Geology*, 18(4) : 423 – 439
- Hoskin PWO and Schaltegger U. 2003. The composition of zircon and igneous and metamorphic petrogenesis. *Reviews in Mineralogy and Geochemistry*, 53(1) : 27 – 62
- Hu RZ, Peng JT, Ma DS, Su WC, Shi CH, Bi XW and Tu GC. 2007. Epoch of large-scale low-temperature mineralizations in southwestern Yangtze massif. *Mineral Deposits*, 26(6) : 583 – 596 (in Chinese with English abstract)
- Hu RZ and Zhou MF. 2012. Multiple Mesozoic mineralization events in South China: An introduction to the thematic issue. *Mineralium Deposita*, 47(6) : 579 – 588
- Hu RZ, Mao JW, Hua RM and Fan WM. 2015. Intra-continental Mineralization of South China Craton. Beijing: Science Press, 1 – 903 (in Chinese)
- Huang YM. 1996. A new clue for gold-searching in Xuefeng tectonic area: A discovery of Au-mineralized lamprophyre in Anhua. *Hunan Geology*, 15(4) : 198 (in Chinese)
- Jiang SY, Wang RC, Xu XS and Zhao KD. 2005. Mobility of high field strength elements (HFSE) in magmatic-, metamorphic-, and submarine-hydrothermal systems. *Physics and Chemistry of the Earth, Parts A/B/C*, 30(17 – 18) : 1020 – 1029
- Kang RH. 2002. Analysis of exploration perspectives of gold-antimony deposits in Baimashan-Longshan EW-striking structural zone, Hunan Province. *Geology and Mineral resources of South China*, (1) : 57 – 61 (in Chinese with English abstract)
- Li HQ, Wang DH, Chen FW, Mei YP and Cai H. 2008. Study on chronology of the Chanziping and Daping gold deposit in Xuefeng Mountains, Hunan Province. *Acta Geologica Sinica*, 82(7) : 900 – 905 (in Chinese with English abstract)
- Li JH, Wu JC and Li YG. 2007. The ore-controlling factors of Baimashan-Longshan gold-stibium belt and metallogenetic prognosis. *Resources Environment & Engineering*, 21(Suppl.) : 33 – 36 (in Chinese with English abstract)
- Li JH, Zhang YQ, Xu XB, Li HL, Dong SW and Li TD. 2014. SHRIMP U-Pb dating of zircons from the Baimashan Longtan super-unit and Wawutang granites in Hunan Province and its geological implication. *Journal of Jilin University (Earth Science Edition)*, 44(1) : 158 – 175 (in Chinese with English abstract)
- Liang HY. 1989. Ore material sources of the Longshan gold-antimony deposit. *Mineral Deposits*, 8(4) : 39 – 48 (in Chinese with English abstract)
- Liang HY. 1991. Geochemistry of ore fluids and genesis of Longshan Au-Sb deposit, west Hunan, China. *Geochimica*, 20(4) : 342 – 350 (in Chinese with English abstract)
- Liu JS. 1993. On the mineralization epoch of Xuefeng metallogenetic province. *Gold*, 14(7) : 7 – 12 (in Chinese with English abstract)
- Liu JS. 1996. Relationship between felsic dikes and antimony-gold mineralization in central Hunan. *Geological Exploration for Non-Ferrous Metals*, 5(6) : 321 – 326 (in Chinese with English abstract)
- Liu K, Mao JR, Zhao XL, Ye HM and Hu Q. 2014. Geological and geochemical characteristics and genetic significance of the Ziyunshan pluton in Hunan Province. *Acta Geologica Sinica*, 88(2) : 208 – 227 (in Chinese with English abstract)
- Liu PC, Tang QG and Li HC. 2008. Geological characteristics, enrichment laws and prospecting direction of gold-antimony deposit in Longshan deposits of Hunan. *Geology and Prospecting*, 44(4) : 31 – 38 (in Chinese with English abstract)
- Liu SY, Bao ZX and Bao JM. 2013. Gold deposit features and metallogenetic regularity of Precambrian in Hunan Province, China. *Geology and Mineral Resources of South China*, 29(1) : 37 – 45 (in Chinese with English abstract)
- Liu YS, Hu ZC, Gao S, Günther D, Xu J, Gao CG and Chen HH. 2008. In situ analysis of major and trace elements of anhydrous minerals by LA-ICP-MS without applying an internal standard. *Chemical Geology*, 257(1 – 2) : 34 – 43
- Lu XW. 1999. Regional ore-controlling characteristics of gold and antimony deposits in central Hunan. *Uranium Geology*, 15(6) : 344 – 349 (in Chinese with English abstract)
- Ludwig KR. 2003. Isoplot/Ex version 3.00: A geochronology toolkit for Microsoft Excel. Berkeley Geochronology Center Special Publication, 4 : 1 – 70
- Luo GY. 1994. Geologic features of granite-porphyry dykes in Liaojiaping district and the relationship with W, Sb, Au mineralization. *Hunan Geology*, 13(1) : 7 – 10 (in Chinese with English abstract)
- Luo XL. 1989. On the epoch of the formation of Precambrian gold deposits in Hunan province. *Journal of Guilin College of Geology*, 9(1) : 25 – 34 (in Chinese with English abstract)
- Ma DS, Pan JY, Xie QL and He J. 2002. Ore source of Sb (Au) deposits in Central Hunan: I. Evidences of trace elements and experimental geochemistry. *Mineral Deposits*, 21(3) : 366 – 376 (in Chinese with English abstract)
- Ma DS, Pan JY and Xie QL. 2003. Ore sources of Sb (Au) deposits in Central Hunan: II. Evidence of isotopic geochemistry. *Mineral Deposits*, 22(1) : 78 – 87 (in Chinese with English abstract)
- Mao JR, Ye HM, Liu K, Li ZL, Takahashi Y, Zhao XL and Kee WS. 2013. The Indosinian collision-extension event between the South China Block and the Palaeo-Pacific Plate: Evidence from Indosinian alkaline granitic rocks in Dashuang, eastern Zhejiang, South China. *Lithos*, 172 – 173 : 81 – 97
- Mao JR, Li ZL and Ye HM. 2014. Mesozoic tectono-magmatic activities in South China: Retrospect and prospect. *Science China (Earth Sciences)*, 57(12) : 2853 – 2877
- Mao JW and Li HY. 1997. Research on genesis of the gold deposits in the Jiangnan terrain. *Geochimica*, 26(5) : 71 – 81 (in Chinese with English abstract)
- Miller DA and White RA. 1998. A conterminous United States multilayer soil characteristics dataset for regional climate and hydrology modeling. *Earth Interactions*, 2(2) : 1 – 26
- Pang BC, Yang DS, Zhou Z, Liu YM, Liu PC and Liu YD. 2011. Trace elements in pyrites and their implication for hydrothermal ore-forming process in Longshan gold-antimony deposits, Hunan, China. *Geoscience*, 25(5) : 832 – 845 (in Chinese with English abstract)
- Pearce JA, Harris NBW and Tindle AG. 1984. Trace element discrimination diagrams for the tectonic interpretation of granitic rocks. *Journal of Petrology*, 25(4) : 956 – 983

- Pei RF, Wu LS and Xiong QR. 1998. Metallogenic Preferentiality and Exceptional Metallotect Convergence of Giant Ore Deposits in China. Beijing: Geological Publishing House, 1–418 (in Chinese)
- Peng B and Chen GH. 2000. Phenomena and formation mechanism for metallogenetic explosion of Sb-Au ore deposits in Hunan Province, China. *Geotectonica et Metallogenesis*, 24 (4): 357–364 (in Chinese with English abstract)
- Peng B and Frei R. 2004. Nd-Sr-Pb isotopic constraints on metal and fluid sources in W-Sb-Au mineralization at Woxi and Liaojiaping (western Hunan, China). *Mineralium Deposita*, 39(3): 313–327
- Peng JT and Hu RZ. 2001. Metallogenic epoch and metallogenetic tectonic environment of antimony deposits, South China. *Geology-Geochemistry*, 29 (3): 104–108 (in Chinese with English abstract)
- Peng JT, Hu RZ, Zou LQ and Liu JX. 2002. Isotope tracing of ore-forming materials for the Xikuangshan antimony deposit, Central Hunan. *Acta Mineralogica Sinica*, 22(2): 155–159 (in Chinese with English abstract)
- Peng JT, Hu RZ and Burnard PG. 2003. Samarium-neodymium isotope systematics of hydrothermal calcites from the Xikuangshan antimony deposit (Hunan, China): The potential of calcite as a geochronometer. *Chemical Geology*, 200(1–2): 129–136
- Shi MK, Fu BQ, Jin XX and Zhou XC. 1994. Antimony Metallogenesis in Central Part of Hunan Province. Changsha: Hunan Press of Science and Technology, 1–151 (in Chinese)
- Sun JM, Lou YL, Gao LJ and Bao ZX. 2007. Geology and metallogenesis of Precambrian gold deposits in central Hunan Province. *Geology and Resources*, 16(3): 189–195 (in Chinese with English abstract)
- Sun SS and McDonough WF. 1989. Chemical and isotopic systematics of oceanic basalts: Implications for mantle composition and processes. In: Saunders AD and Norry MJ (eds.). *Magma in the Ocean Basins*. Geological Society, London, Special Publications, 42(1): 313–345
- Sun T, Zhou XM, Chen PR, Li HM, Zhou HY, Wang ZC and Sheng WZ. 2003. Genesis and tectonic significance of the Mesozoic strongly peraluminous granitoid in southern Nanling. *Science in China (Series D)*, 33(12): 1209–1218 (in Chinese)
- Sun T. 2006. A new map showing the distribution of granites in South China and its explanatory notes. *Geological Bulletin of China*, 25 (3): 332–335 (in Chinese with English abstract)
- Sylvester PJ. 1998. Post-collisional strongly peraluminous granites. *Lithos*, 45(1–4): 29–44
- Tang CH. 2012. Geological and geochemical characteristics of Hunan Longshan gold deposit and resource forecast. *Geology of Chemical Minerals*, 34(2): 90–94 (in Chinese with English abstract)
- Tao Y, Gao ZM, Jin JF and Zeng LJ. 2001. The origin of ore-forming fluid of Xikuangshan-type antimony deposits in Central Hunan Province. *Geology-Geochemistry*, 29(1): 14–20 (in Chinese with English abstract)
- Taylor SR and McLennan SM. 1985. The Continental Crust: Its Composition and Evolution. Oxford: Blackwell, 1–328
- Tu GC. 2002. Two unique mineralization areas in southwest China. *Bulletin of Mineralogy, Petrology and Geochemistry*, 21(1): 1–2 (in Chinese with English abstract)
- Vervoort JD, Patchett PJ, Gehrels GE and Nutman AP. 1996. Constraints on early Earth differentiation from hafnium and neodymium isotopes. *Nature*, 379(6566): 624–627
- Vervoort JD and Blachert-Toft J. 1999. Evolution of the depleted mantle: Hf isotope evidence from juvenile rocks through time. *Geochimica et Cosmochimica Acta*, 63(3–4): 533–556
- Wang Q, Zhu DC, Zhao ZD, Guan Q, Zhang XQ, Sui QL, Hu ZC and Mo XX. 2012. Magmatic zircons from I-, S- and A-type granitoids in Tibet: Trace element characteristics and their application to detrital zircon provenance study. *Journal of Asian Earth Sciences*, 53: 59–66
- Wang YJ, Fan WM, Liang XQ, Peng TP and Shi YR. 2005. SHRIMP zircon U-Pb geochronology of Indosian granites in Hunan Province and its petrogenetic implications. *Chinese Science Bulletin*, 50 (13): 1395–1403
- Wang YJ, Fan WM, Sun M, Liang XQ, Zhang YH and Peng TP. 2007. Geochronological, geochemical and geothermal constraints on petrogenesis of the Indosian peraluminous granites in the South China Block: A case study in the Hunan Province. *Lithos*, 96(3–4): 475–502
- Wang YJ, Fan WM, Zhang GW and Zhang YH. 2013. Phanerozoic tectonics of the South China Block: Key observations and controversies. *Gondwana Research*, 23(4): 1273–1305
- Wang ZX. 1988. On the metallogeny of the Longshan Au-Sb deposit. *Geology and Prospecting*, (12): 6–12 (in Chinese with English abstract)
- Wu FY, Li XH, Zheng YF and Gao S. 2007. Lu-Hf isotopic systematics and their applications in petrology. *Acta Petrologica Sinica*, 23(2): 185–220 (in Chinese with English abstract)
- Wu JC, Wang JR, Wu CJ and Jia ZL. 2007. Fracture tectonic geochemical characteristics of gold deposit in Longshan area of Hunan. *Mineral Resources and Geology*, 21(3): 351–357 (in Chinese with English abstract)
- Wu LS and Hu XW. 2000. Xikuangshan mica-plagioclase lamprophyre and its granite inclusions, Hunan Province. *Geology-Geochemistry*, 28(2): 51–55 (in Chinese with English abstract)
- Wu YB and Zheng YF. 2004. Genesis of zircon and its constraints on interpretation of U-Pb age. *Chinese Science Bulletin*, 49(15): 1554–1569
- Wu YJ. 2003. The metallogenic regularity, structure and prognosticate of Longshan Au-Sb deposit in Hunan Province. Master Degree Thesis. Changsha: Central South University (in Chinese with English summary)
- Xiao QM, Zeng DR, Jin FQ, Yang MY and Yang ZF. 1992. Time-space distribution feature and exploration guide of China's Sb deposits. *Geology and Prospecting*, 28(12): 9–14 (in Chinese with English abstract)
- Yao ZK and Zhu RB. 1993. Polygenetic compound model for the Fuzhuxi gold deposit of Hunan Province and its prospecting. *Geotectonica et Metallogenesis*, 17(3): 199–209 (in Chinese with English abstract)
- Yu JH, Wang LJ, Wang XL, Qiu JS and Zhao L. 2007. Geochemistry and geochronology of the Fucheng Complex in the southeastern Jiangxi Province, China. *Acta Petrologica Sinica*, 23(6): 1441–1456 (in Chinese with English abstract)
- Zhang XN. 2016. Ore control structure of the Longshan Au-Sb deposit. *Acta Geologica Sichuan*, 36 (2): 243–246 (in Chinese with English abstract)
- Zhang ZY, Xie GQ, Zhu QQ, Li W, Han YX and Wang FL. 2016. Mineralogical characteristics of skarns of Caojiaiba large tungsten deposit in central Hunan Province and their geological significance. *Mineral Deposits*, 35 (2): 335–348 (in Chinese with English abstract)
- Zhao JH, Peng JT, Hu RZ and Fu YZ. 2005. Chronology, petrology, geochemistry and tectonic environment of Banxi quartz porphyry dikes, Hunan Province. *Acta Geoscientica Sinica*, 26(6): 525–534 (in Chinese with English abstract)
- Zhao KD, Jiang SY, Chen WF, Chen PR and Ling HF. 2013. Zircon U-Pb chronology and elemental and Sr-Nd-Hf isotope geochemistry of two Triassic A-type granites in South China: Implication for petrogenesis and Indosian transtensional tectonism. *Lithos*, 160–161: 292–306
- Zhao ZX, Xu ZW, Miao BH, Zuo CH, Lu JJ, Lu R and Chen JQ. 2015. Diagenetic age and material source of the Guandimiao granitic batholith, Hengyang city, Hunan Province. *Acta Geologica Sinica*, 89(7): 1219–1230 (in Chinese with English abstract)
- Zheng SG. 2006. Geological characteristics of Longshan gold antimony deposit and resource forecast. *Geology and Mineral Resources of South China*, (4): 14–21, 80 (in Chinese with English abstract)
- Zhou XM, Sun T, Shen WZ, Shu LS and Niu YL. 2006. Petrogenesis of Mesozoic granitoids and volcanic rocks in South China: A response to tectonic evolution. *Episodes*, 29(1): 26–33

附中文参考文献

- 柏道远, 钟响, 贾朋远, 熊雄, 黄文义. 2014. 湘中印支期关帝庙岩体地球化学特征及成因. 沉积与特提斯地质, 34(4): 92–104
- 鲍肖, 陈放. 1995. 湖南龙山锑金矿床成矿规律与成因探讨. 湖南冶金, (6): 24–28, 46
- 鲍肖, 万溶江, 包觉敏. 2000. 湘中前寒武系锑砷金矿床地质特征及找矿标志. 湖南冶金, (5): 34–39
- 鲍振襄, 万榕江, 鲍珏敏. 2002. 湖南前寒武系地层中长英质脉岩与金成矿关系. 黄金地质, 8(1): 33–39
- 陈卫锋, 陈培荣, 黄宏业, 丁兴, 孙涛. 2007. 湖南白马山岩体花岗岩及其包体的年代学和地球化学研究. 中国科学(D辑), 37(7): 873–893
- 陈小明, 王汝成, 刘昌实, 胡欢, 张文兰, 高剑锋. 2002. 广东从化佛冈(主体)黑云母花岗岩定年和成因. 高校地质学报, 8(3): 293–307
- 陈新跃, 尹萍, 匡文龙, 戴德求, 资锋. 2012. 湘西雪峰地区金多金属成矿带研究进展. 地质科技情报, 31(3): 82–88
- 丁兴, 陈培荣, 陈卫锋, 黄宏业, 周新民. 2005. 湖南沩山花岗岩中锆石 LA-ICPMS U-Pb 定年: 成岩启示和意义. 中国科学(D辑), 35(7): 606–616
- 丁兴, 孙卫东, 汪方跃, 陈林丽, 李秋立, 陈福坤. 2012. 湖南沩山岩体多期云母的 Rb-Sr 同位素年龄和矿物化学组成及其成岩成矿指示意义. 岩石学报, 28(12): 3823–3840
- 付山岭, 胡瑞忠, 陈佑纬, 骆金诚. 2016. 湘中龙山大型金锑矿床成矿时代研究——黄铁矿 Re-Os 和锆石 U-Th/He 定年. 岩石学报, 32(11): 3507–3517
- 关俊雷, 耿全如, 王国芝, 彭智敏, 张璋, 寇福德, 丛峰, 李娜. 2014. 北冈底斯带日土县-拉梅拉山口花岗岩体的岩石地球化学特征, 锆石 U-Pb 测年及 Hf 同位素组成. 岩石学报, 30(6): 1666–1684
- 贺文华, 康如华, 刘大勇, 马武良, 谢彪武, 胡绪云. 2015. 湖南省阳县龙山金锑矿区构造控矿规律及找矿方向. 华南地质与矿产, 31(3): 261–267
- 胡瑞忠, 彭建堂, 马东升, 苏文超, 施春华, 毕献武, 涂光炽. 2007. 扬子地块西南缘大面积低温成矿时代. 矿床地质, 26(6): 583–596
- 胡瑞忠, 毛景文, 华仁民, 范蔚茗. 2015. 华南陆块陆内成矿作用. 北京: 科学出版社, 1–903
- 湖南省地质矿产局. 1988. 湖南省区域地质志. 北京: 地质出版社, 1–467
- 黄石明. 1996. 雪峰构造区的找金新线索: 安化发现煌斑岩型金矿化. 湖南地质, 15(4): 198
- 康如华. 2002. 湖南白马山-龙山东西向构造带金锑矿找矿前景分析. 华南地质与矿产, (1): 57–61
- 李华芹, 王登红, 陈富文, 梅玉萍, 蔡红. 2008. 湖南雪峰山地区铲子坪和大坪金矿成矿作用年代学研究. 地质学报, 82(7): 900–905
- 李已华, 吴继承, 李永光. 2007. 湖南白马山-龙山金锑矿带控矿因素与成矿预测. 资源环境与工程, 21(增): 33–36
- 李建华, 张岳桥, 徐先兵, 李海龙, 董树文, 李廷栋. 2014. 湖南白山龙潭超单元瓦屋塘花岗岩锆石 SHRIMP U-Pb 年龄及其地质意义. 吉林大学学报(地球科学版), 44(1): 158–175
- 梁华英. 1989. 龙山金锑矿床成矿物质来源研究. 矿床地质, 8(4): 39–48
- 梁华英. 1991. 龙山金锑矿床成矿流体地球化学和矿床成因研究. 地球化学, 20(4): 342–350
- 刘继顺. 1993. 关于雪峰山一带金成矿区的成矿时代. 黄金, 14(7): 7–12
- 刘继顺. 1996. 湘中地区长英质脉岩与锑(金)成矿关系. 有色金属矿产与勘查, 5(6): 321–326
- 刘凯, 毛建仁, 赵希林, 叶海敏, 胡青. 2014. 湖南紫云山岩体的地质地球化学特征及其成因意义. 地质学报, 88(2): 208–227
- 刘鹏程, 唐清国, 李惠纯. 2008. 湖南龙山矿区金锑矿地质特征、富集规律与找矿方向. 地质与勘探, 44(4): 31–38
- 刘升友, 鲍振襄, 鲍珏敏. 2013. 湖南前寒武系金矿特征及成矿规律. 华南地质与矿产, 29(1): 37–45
- 卢新卫. 1999. 湘中金、锑矿床区域控矿特征研究. 铀矿地质, 15(6): 344–349
- 罗纲元. 1994. 廖家坪地区花岗斑岩地质特征及其与钨锑金成矿的关系. 湖南地质, 13(1): 7–10
- 罗献林. 1989. 论湖南前寒武系金矿床的形成时代. 桂林冶金地质学院学报, 9(1): 25–34
- 马东升, 潘家永, 解庆林, 何江. 2002. 湘中锑(金)矿床成矿物质来源-I. 微量元素及其实验地球化学证据. 矿床地质, 21(3): 366–376
- 马东升, 潘家永, 解庆林. 2003. 湘中锑(金)矿床成矿物质来源-II. 同位素地球化学证据. 矿床地质, 22(1): 78–87
- 毛景文, 李红艳. 1997. 江南古陆某些金矿床成因讨论. 地球化学, 26(5): 71–81
- 庞保成, 杨东生, 周志, 刘义茂, 刘鹏程, 刘远栋. 2011. 湖南龙山金锑矿黄铁矿微量元素特征及其对成矿过程的指示. 现代地质, 25(5): 832–845
- 裴荣富, 吴良士, 熊群尧. 1998. 中国特大型矿床成矿偏在性与异常成矿构造聚敛场. 北京: 地质出版社, 1–418
- 彭渤, 陈广浩. 2000. 湖南锑金矿成矿大爆发: 现象与机制. 大地构造与成矿学, 24(4): 357–364
- 彭建堂, 胡瑞忠. 2001. 华南锑矿带的成矿时代和成矿构造环境. 地质地球化学, 29(3): 104–108
- 彭建堂, 胡瑞忠, 邹利群, 刘建雄. 2002. 湘中锡矿山锑矿床成矿物质来源的同位素示踪. 矿物学报, 22(2): 155–159
- 史明魁, 傅必勤, 靳西祥, 周雪昌. 1994. 湘中锑矿. 长沙: 湖南科学技术出版社, 1–151
- 孙际茂, 娄亚利, 高利军, 鲍振襄. 2007. 湘中前寒武系金矿地质及相关成矿问题探讨. 地质与资源, 16(3): 189–195
- 孙涛, 周新民, 陈培荣, 李惠民, 周红英, 王志成, 沈渭洲. 2003. 南岭东段中生代强过铝花岗岩成因及其大地构造意义. 中国科学(D辑), 33(12): 1209–1218
- 孙涛. 2006. 新编华南花岗岩分布图及其说明. 地质通报, 25(3): 332–335

- 唐朝晖. 2012. 湖南龙山金矿床地质-地球化学特征及找矿预测. 化工矿产地质, 34(2): 90–94
- 陶琰, 高振敏, 金景福, 曾令交. 2001. 湘中锡矿山式锑矿成矿物质来源探讨. 地质地球化学, 29(1): 14–20
- 涂光炽. 2002. 我国西南地区两个别具一格的成矿带(域). 矿物岩石地球化学通报, 21(1): 1–2
- 王岳军, 范蔚茗, 梁新权, 彭头平, 石玉若. 2005. 湖南印支期花岗岩 SHRIMP 锆石 U-Pb 年龄及其成因启示. 科学通报, 50(12): 1259–1266
- 王中雄. 1988. 龙山金锑矿床几个成矿问题初探. 地质与勘探, (12): 6–12
- 吴福元, 李献华, 郑永飞, 高山. 2007. Lu-Hf 同位素体系及其岩石学应用. 岩石学报, 23(2): 185–220
- 吴继承, 王金荣, 吴春俊, 贾志磊. 2007. 湖南龙山地区金矿床断裂构造地球化学特征. 矿产与地质, 21(3): 351–357
- 吴良士, 胡雄伟. 2000. 湖南锡矿山地区云斜煌斑岩及其花岗岩包体的意义. 地质地球化学, 28(2): 51–55
- 吴元保, 郑永飞. 2004. 锆石成因矿物学研究及其对 U-Pb 年龄解释的制约. 科学通报, 49(16): 1589–1604
- 吴运军. 2003. 湖南省新邵县龙山金锑矿成矿规律及深边部成矿预测. 硕士学位论文. 长沙: 中南大学
- 肖启明, 曾笃仁, 金富秋, 杨明跃, 阳志芳. 1992. 中国锑矿床时空分布规律及找矿方向. 地质与勘探, 28(12): 9–14
- 姚振凯, 朱蓉斌. 1993. 湖南符竹溪金矿床多因复成模式及其找矿意义. 大地构造与成矿学, 17(3): 199–209
- 于津海, 王丽娟, 王孝磊, 邱检生, 赵蕾. 2007. 赣东南富城杂岩体的地球化学和年代学研究. 岩石学报, 23(6): 1441–1456
- 张新念. 2016. 龙山金锑矿控矿构造特征. 四川地质学报, 36(2): 243–246
- 张志远, 谢桂青, 朱乔乔, 李伟, 韩颖霄, 王凤兰. 2016. 湘中曹家坝大型钨矿床的主要矽卡岩矿物学特征及其地质意义. 矿床地质, 35(2): 335–348
- 赵军红, 彭建堂, 胡瑞忠, 符亚洲. 2005. 湖南板溪脉岩的年代学、岩石学、地球化学及其构造环境. 地球学报, 26(6): 525–534
- 赵增霞, 徐兆文, 缪柏虎, 左昌虎, 陆建军, 路睿, 陈进全. 2015. 湖南衡阳关帝庙花岗岩岩基形成时代及物质来源探讨. 地质学报, 89(7): 1219–1230
- 郑时干. 2006. 龙山金锑矿地质特征及深部找矿预测. 华南地质与矿产, (4): 14–21, 80

附表 1 岩脉的锆石稀土元素含量 ($\times 10^{-6}$)Attached Table 1 The rare earth element data ($\times 10^{-6}$) of zircons from dykes

| 测点号 | La | Ce | Pr | Nd | Sm | Eu | Gd | Tb | Dy | Ho | Er | Tm | Yb | Lu | Y | Nb | Pb | Hf | Th | U | Σ REE | LREE | HREE | δ Eu | δ Ce | U/Yb | (Nb/Pb) _N |
|-----------|-----|------|-----|-----|-----|-----|------|------|------|------|-----|------|-----|-------|------|-----|------|-------|-----|------|--------------|------|------|-------------|-------------|--------|----------------------|
| ZW-01-03 | 1.0 | 16.6 | 1.4 | 9.3 | 7.3 | 2.3 | 26.2 | 7.9 | 91.1 | 32.9 | 153 | 32.2 | 336 | 60.9 | 1073 | 3.3 | 139 | 11131 | 248 | 789 | 778 | 37.9 | 740 | 0.5 | 2.9 | 2.3 | 0.2 |
| ZW-01-04 | 1.3 | 10.5 | 0.5 | 3.4 | 4.2 | 0.4 | 20.4 | 7.2 | 89.7 | 34.9 | 163 | 34.6 | 343 | 65.4 | 1107 | 3.3 | 20.2 | 11441 | 250 | 463 | 778 | 20.2 | 758 | 0.1 | 3.4 | 1.4 | 1.6 |
| ZW-01-05 | 0.1 | 5.0 | 0.1 | 1.6 | 2.6 | 0.4 | 17.7 | 6.4 | 78.4 | 31.5 | 150 | 31.9 | 320 | 61.1 | 977 | 2.8 | 11.7 | 11109 | 139 | 261 | 706 | 9.7 | 697 | 0.1 | 13.3 | 0.8 | 2.4 |
| ZW-01-06 | 0.0 | 5.7 | 0.1 | 2.7 | 5.1 | 0.5 | 27.2 | 9.6 | 121 | 48.2 | 232 | 49 | 496 | 95.8 | 1545 | 3.4 | 14.2 | 10263 | 172 | 305 | 1093 | 14.1 | 1079 | 0.1 | 14.2 | 0.6 | 2.4 |
| ZW-01-07 | 3.2 | 19 | 1.0 | 5.2 | 4.7 | 1.0 | 27.2 | 10.7 | 143 | 60.6 | 316 | 73.8 | 820 | 167.9 | 2067 | 3.6 | 47.3 | 11217 | 169 | 335 | 1653 | 34.2 | 1618 | 0.2 | 2.6 | 0.4 | 0.8 |
| ZW-01-08 | 0.0 | 5.3 | 0.2 | 3.4 | 6.2 | 0.8 | 30.6 | 9.8 | 112 | 42.3 | 183 | 36.8 | 360 | 65.8 | 1315 | 2.1 | 10.1 | 9307 | 171 | 199 | 856 | 15.9 | 840 | 0.1 | 6.9 | 0.6 | 2.1 |
| ZW-01-09 | 0.1 | 7.2 | 0.1 | 1.5 | 4.0 | 0.5 | 23.0 | 8.4 | 105 | 41.8 | 198 | 42.3 | 422 | 79.6 | 1351 | 3.6 | 21.5 | 10893 | 237 | 478 | 934 | 13.4 | 920 | 0.1 | 12.6 | 1.1 | 1.7 |
| ZW-01-10 | 3.9 | 18.9 | 1.7 | 9.9 | 7.7 | 1.1 | 31.4 | 10.9 | 130 | 49.8 | 228 | 49.1 | 492 | 89.1 | 1657 | 4.3 | 34.8 | 11290 | 315 | 671 | 1123 | 43.1 | 1080 | 0.2 | 1.8 | 1.4 | 1.2 |
| ZW-01-12 | 0.1 | 6.7 | 0.1 | 1.4 | 3.5 | 0.4 | 21.1 | 7.8 | 98.3 | 39.6 | 188 | 41.1 | 426 | 78.9 | 1264 | 3.5 | 22.8 | 11518 | 230 | 525 | 913 | 12.1 | 901 | 0.1 | 18.8 | 1.2 | 1.6 |
| ZW-01-14 | 0.5 | 7.7 | 0.3 | 2.3 | 4.0 | 0.4 | 22.5 | 8.2 | 104 | 41.9 | 195 | 41.8 | 424 | 79.3 | 1312 | 3.5 | 18.8 | 11252 | 239 | 430 | 932 | 15.2 | 917 | 0.1 | 4.8 | 1.0 | 1.9 |
| ZW-01-15 | 0.1 | 17.9 | 0.3 | 4.4 | 7.3 | 1.4 | 35.8 | 11.9 | 151 | 57.1 | 267 | 53.1 | 542 | 98.1 | 1803 | 1.8 | 39.9 | 10369 | 222 | 254 | 1248 | 31.4 | 1217 | 0.2 | 19.8 | 0.5 | 0.4 |
| ZW-01-17 | 0.1 | 5.3 | 0.2 | 3.0 | 5.0 | 0.6 | 22.9 | 7.5 | 95.6 | 36.2 | 173 | 35.8 | 375 | 69.3 | 1127 | 2 | 13 | 9999 | 140 | 284 | 830 | 14.3 | 816 | 0.2 | 5.9 | 0.8 | 1.6 |
| ZW-01-19 | 0.0 | 6.3 | 0.1 | 1.9 | 3.8 | 0.5 | 23.7 | 8.4 | 109 | 42.4 | 207 | 42.9 | 452 | 82.5 | 1309 | 2.9 | 20.2 | 11293 | 210 | 473 | 980 | 12.7 | 967 | 0.1 | 13.5 | 1.0 | 1.5 |
| ZW-01-20 | 0.0 | 4.7 | 0.1 | 1.7 | 3.5 | 0.4 | 21.8 | 7.4 | 95 | 36.6 | 178 | 36 | 384 | 71.3 | 1132 | 2.1 | 12 | 11132 | 145 | 268 | 840 | 10.4 | 830 | 0.1 | 17 | 0.7 | 1.7 |
| ZW-01-22 | 0.1 | 9.8 | 0.3 | 5.6 | 9.8 | 1.5 | 46.7 | 14.1 | 162 | 56.1 | 247 | 46.2 | 460 | 80.6 | 1637 | 1.6 | 16.0 | 11018 | 363 | 307 | 1140 | 27.1 | 1113 | 0.2 | 7.7 | 0.7 | 1.0 |
| SXC-02-01 | 1.6 | 12.1 | 0.7 | 5.4 | 7.3 | 0.6 | 33.7 | 11.5 | 139 | 52.7 | 239 | 49.6 | 489 | 89.1 | 1674 | 3.3 | 27 | 11815 | 362 | 577 | 1131 | 27.8 | 1103 | 0.1 | 2.8 | 1.2 | 1.2 |
| SXC-02-04 | 0.4 | 9.5 | 0.3 | 2.6 | 5.1 | 0.4 | 31.3 | 11.3 | 143 | 57.5 | 270 | 55.6 | 568 | 104 | 1856 | 4.5 | 27.9 | 11636 | 348 | 639 | 1258 | 18.2 | 1240 | 0.1 | 7.3 | 1.1 | 1.6 |
| SXC-02-05 | 0.7 | 8.7 | 0.3 | 2.5 | 3.5 | 0.3 | 21.9 | 7.8 | 102 | 41.2 | 198 | 42.9 | 443 | 83.2 | 1316 | 3.8 | 25.8 | 12042 | 268 | 651 | 956 | 16.1 | 940 | 0.1 | 4.3 | 1.5 | 1.5 |
| SXC-02-06 | 1.4 | 11.5 | 0.6 | 4.7 | 6.0 | 0.6 | 30.4 | 11.0 | 136 | 53.5 | 250 | 52.3 | 524 | 96.5 | 1744 | 3.5 | 25.7 | 11647 | 340 | 583 | 1179 | 24.8 | 1154 | 0.1 | 3.0 | 1.1 | 1.4 |
| SXC-02-08 | 0.0 | 3.4 | 0.1 | 1.6 | 3.7 | 0.3 | 19.1 | 6.6 | 81.7 | 32.2 | 152 | 32.2 | 332 | 62.6 | 1014 | 2.0 | 8.0 | 10336 | 109 | 190 | 727 | 9.1 | 718 | 0.1 | 11.2 | 0.6 | 2.6 |
| SXC-02-09 | 2.2 | 16.1 | 0.8 | 5.0 | 5.1 | 0.6 | 26.5 | 9.5 | 122 | 48.1 | 219 | 46.4 | 469 | 85.3 | 1535 | 4.1 | 23.4 | 10323 | 297 | 528 | 1056 | 29.9 | 1026 | 0.1 | 2.9 | 1.1 | 1.7 |
| SXC-02-10 | 0.0 | 6.7 | 0.1 | 1.5 | 3.6 | 0.3 | 24.2 | 9.9 | 133 | 54.7 | 270 | 59.1 | 619 | 115 | 1827 | 4.9 | 30.7 | 12061 | 249 | 757 | 1297 | 12.3 | 1284 | 0.1 | 15.7 | 1.2 | 1.6 |
| SXC-02-11 | 0.3 | 10.2 | 0.3 | 2.4 | 5.0 | 0.6 | 27.2 | 9.7 | 125 | 49.7 | 230 | 48.9 | 495 | 91.2 | 1588 | 4.3 | 33 | 11294 | 390 | 765 | 1095 | 18.8 | 1076 | 0.1 | 8.1 | 1.5 | 1.3 |
| SXC-02-12 | 0.1 | 6.6 | 0.1 | 1.7 | 3.4 | 0.3 | 20.6 | 7.5 | 91.7 | 36.9 | 174 | 37.9 | 388 | 72.2 | 1174 | 3.2 | 18 | 11655 | 214 | 445 | 841 | 12.3 | 829 | 0.1 | 12.2 | 1.1 | 1.8 |
| SXC-02-13 | 3.1 | 18.7 | 1.6 | 9.4 | 7.6 | 1.1 | 30.0 | 11.5 | 144 | 54.6 | 254 | 53.6 | 547 | 100 | 1761 | 5.2 | 47.8 | 11677 | 507 | 1226 | 1237 | 41.5 | 1195 | 0.2 | 2.0 | 2.2 | 1.1 |
| SXC-02-14 | 1.0 | 10.5 | 1.0 | 7.3 | 7.3 | 1.8 | 28.1 | 10.7 | 130 | 47.7 | 219 | 46.5 | 463 | 84.7 | 1563 | 4.0 | 24.3 | 11560 | 250 | 598 | 1058 | 28.8 | 1030 | 0.3 | 2.3 | 1.3 | 1.7 |
| SXC-02-15 | 0.4 | 8.2 | 0.4 | 3.0 | 4.4 | 0.7 | 20.0 | 6.8 | 85.8 | 31.1 | 147 | 29.4 | 305 | 53.1 | 994 | 2.5 | 69.5 | 11581 | 349 | 1000 | 695 | 17.0 | 678 | 0.2 | 4.7 | 3.3 | 0.4 |
| SXC-02-18 | 0.0 | 4.5 | 0.1 | 2.2 | 4.8 | 0.5 | 25.6 | 8.5 | 110 | 41.1 | 199 | 39.1 | 410 | 75 | 1311 | 1.9 | 12.3 | 9993 | 161 | 254 | 921 | 12.1 | 909 | 0.1 | 15.0 | 0.6 | 1.5 |
| SZ-08-05 | 0.0 | 5.4 | 0.2 | 2.6 | 5.7 | 0.7 | 27.8 | 9.1 | 109 | 42.7 | 195 | 38.9 | 397 | 72.5 | 1348 | 2.4 | 12 | 9923 | 186 | 250 | 907 | 14.6 | 893 | 0.1 | 9.8 | 0.6 | 2.0 |
| SZ-08-06 | 0.0 | 8.7 | 0.1 | 2.2 | 3.9 | 0.6 | 23.3 | 8.4 | 107 | 42.6 | 201 | 42.9 | 434 | 81.4 | 1384 | 3.3 | 19.5 | 10664 | 267 | 434 | 956 | 15.5 | 941 | 0.1 | 19.8 | 1.0 | 1.7 |
| SZ-08-07 | 0.2 | 5.7 | 0.2 | 2.8 | 5.5 | 0.8 | 29.5 | 9.9 | 119 | 47.9 | 220 | 46.0 | 459 | 86.9 | 1557 | 2.2 | 10.8 | 9516 | 163 | 236 | 1034 | 15.3 | 1018 | 0.1 | 5.3 | 0.5 | 2.0 |
| SZ-08-08 | 0.1 | 6.7 | 0.2 | 1.8 | 3.4 | 0.4 | 24.0 | 8.5 | 103 | 41.0 | 188 | 39.8 | 410 | 75.4 | 1301 | 3.0 | 20.2 | 11597 | 250 | 470 | 902 | 12.6 | 889 | 0.1 | 12.2 | 1.1 | 1.5 |

续表 1

Continued Attached Table 1

| 测点号 | La | Ce | Pr | Nd | Sm | Eu | Gd | Tb | Dy | Ho | Er | Tm | Yb | Lu | Y | Nb | Pb | Hf | Th | U | ΣREE | LRREE | HREE | δEu | δCe | U/Yb (Nb/Pb) _N | |
|-------------|-----|------|-----|------|------|-----|------|------|------|------|-----|------|-----|------|------|-----|------|-------|-----|------|------|-------|------|-----|------|---------------------------|-----|
| SZ-08-10 | 0.0 | 4.0 | 0.2 | 3.0 | 5.7 | 0.6 | 27.4 | 9.4 | 110 | 42.3 | 193 | 39.4 | 395 | 73.0 | 1343 | 1.7 | 9.5 | 9791 | 149 | 200 | 903 | 13.5 | 889 | 0.1 | 7.3 | 0.5 | 1.8 |
| SZ-08-13 | 0.1 | 5.1 | 0.1 | 1.2 | 3.4 | 0.3 | 19.0 | 6.8 | 90.0 | 36 | 172 | 38.0 | 384 | 72.8 | 1158 | 2.7 | 19.0 | 11955 | 201 | 434 | 828 | 10.2 | 818 | 0.1 | 17.6 | 1.1 | 1.4 |
| SZ-08-14 | 0.5 | 9.2 | 0.3 | 3.4 | 6.0 | 0.7 | 29.8 | 9.6 | 113 | 43.2 | 195 | 39.7 | 397 | 72.8 | 1379 | 3.2 | 13.2 | 10193 | 184 | 247 | 919 | 20.0 | 899 | 0.1 | 6.4 | 0.6 | 2.4 |
| SZ-08-15 | 2.2 | 15.7 | 1.0 | 7.3 | 7.2 | 1.0 | 31.1 | 10.0 | 117 | 44 | 192 | 39.3 | 393 | 72.2 | 1354 | 2.0 | 16.8 | 10587 | 287 | 330 | 933 | 34.4 | 898 | 0.2 | 2.6 | 0.8 | 1.2 |
| SZ-08-19 | 0.9 | 16.1 | 1.6 | 12.7 | 12.6 | 3.0 | 34.9 | 11.5 | 128 | 45.9 | 205 | 42.0 | 423 | 76.6 | 1497 | 4.0 | 40.4 | 11270 | 373 | 778 | 1014 | 46.9 | 968 | 0.4 | 2.5 | 1.8 | 1.0 |
| SZ-08-20 | 0.6 | 9.9 | 0.4 | 5.4 | 9.9 | 1.5 | 43.0 | 13.1 | 145 | 51.2 | 221 | 43.7 | 421 | 76.1 | 1646 | 2.2 | 18.3 | 9809 | 376 | 372 | 1042 | 27.8 | 1014 | 0.2 | 4.9 | 0.9 | 1.2 |
| SZ-08-11 | 0.7 | 6.3 | 0.2 | 2.1 | 4.0 | 0.4 | 21.6 | 7.7 | 91 | 34.7 | 160 | 32.9 | 329 | 61.3 | 1075 | 2.1 | 13.7 | 10692 | 167 | 285 | 752 | 13.8 | 738 | 0.1 | 3.9 | 0.9 | 1.6 |
| SZ-08-24 | 0.6 | 7.3 | 0.2 | 3.3 | 5.3 | 0.6 | 29.0 | 10.1 | 124 | 48.6 | 223 | 46.9 | 466 | 86.7 | 1572 | 2.9 | 17 | 10339 | 209 | 341 | 1051 | 17.4 | 1034 | 0.1 | 4.5 | 0.7 | 1.7 |
| 14LSC-05-01 | 2.0 | 30.5 | 3.2 | 20.7 | 16.8 | 4.1 | 39.7 | 12.6 | 139 | 44.4 | 203 | 40.2 | 428 | 71.7 | 1475 | 5.9 | 53.6 | 11437 | 364 | 1168 | 1056 | 77.4 | 978 | 0.5 | 2.3 | 2.7 | 1.1 |
| 14LSC-05-02 | 2.0 | 17.6 | 2.2 | 15.7 | 13.0 | 3.7 | 40.4 | 13.3 | 150 | 50.1 | 226 | 45.0 | 468 | 80.4 | 1529 | 2.9 | 29.4 | 11423 | 212 | 560 | 1127 | 54.3 | 1073 | 0.5 | 1.8 | 1.2 | 1.0 |
| 14LSC-05-04 | 0.4 | 6.8 | 0.2 | 1.5 | 3.4 | 0.4 | 19.6 | 7.0 | 89.9 | 34.6 | 168 | 34.3 | 365 | 66.0 | 1073 | 2.5 | 20.3 | 11808 | 223 | 433 | 796 | 12.6 | 784 | 0.1 | 6.7 | 1.2 | 1.2 |
| 14LSC-05-05 | 0.2 | 7.5 | 0.3 | 5.1 | 9.1 | 1.0 | 43.7 | 12.7 | 153 | 53.1 | 239 | 46.3 | 484 | 79.0 | 1588 | 1.9 | 18.4 | 10712 | 294 | 388 | 1134 | 23.3 | 1111 | 0.1 | 5.3 | 0.8 | 1.0 |
| 14LSC-05-08 | 1.0 | 12.1 | 0.6 | 6.3 | 8.1 | 1.4 | 39 | 11.9 | 144 | 51.9 | 246 | 49.2 | 530 | 91.6 | 1738 | 8.4 | 43.2 | 11465 | 491 | 1043 | 1193 | 29.6 | 1163 | 0.2 | 3.6 | 2.0 | 1.9 |
| 14LSC-05-11 | 0.5 | 15.1 | 0.9 | 7.4 | 7.1 | 1.4 | 20.4 | 6.9 | 82.8 | 28.9 | 136 | 27.8 | 312 | 51.7 | 979 | 3.3 | 85.3 | 10915 | 201 | 625 | 699 | 32.3 | 666 | 0.3 | 4.4 | 2.0 | 0.4 |
| 14LSC-05-12 | 0.0 | 4.5 | 0.1 | 2.2 | 4.8 | 0.5 | 25.6 | 8.5 | 110 | 41.1 | 199 | 39.1 | 410 | 75.0 | 1311 | 1.9 | 12.3 | 9993 | 161 | 254 | 921 | 12.1 | 909 | 0.1 | 15 | 0.6 | 1.5 |
| 14LSC-05-14 | 0.0 | 6.0 | 0.3 | 5.3 | 8.5 | 1.0 | 43.4 | 13.2 | 160 | 56.3 | 261 | 49.6 | 515 | 90 | 1738 | 1.8 | 13.4 | 10234 | 221 | 255 | 1209 | 21.1 | 1188 | 0.1 | 5.7 | 0.5 | 1.3 |
| 14LSC-05-17 | 0.1 | 9.3 | 0.3 | 3.7 | 5.4 | 1.4 | 22.3 | 6.5 | 77.1 | 26.6 | 125 | 25.1 | 267 | 48.6 | 890 | 1.7 | 18.4 | 11043 | 207 | 438 | 618 | 20.2 | 598 | 0.3 | 7.8 | 1.6 | 0.9 |
| 14LSC-05-19 | 0.3 | 8.7 | 0.3 | 4.5 | 7.5 | 0.8 | 39.8 | 12.8 | 158 | 56.4 | 259 | 49.4 | 506 | 88.6 | 1708 | 2.3 | 21.3 | 10402 | 327 | 425 | 1193 | 22.3 | 1170 | 0.1 | 5.7 | 0.8 | 1.1 |
| WTC-10-01 | 0.2 | 12.8 | 0.3 | 2.9 | 4.2 | 1.2 | 19.2 | 6.8 | 88.5 | 33.1 | 168 | 35.2 | 391 | 69.7 | 1140 | 4.7 | 31.7 | 10185 | 244 | 766 | 833 | 21.5 | 812 | 0.3 | 10.2 | 2.0 | 1.5 |
| WTC-10-02 | 0.1 | 11.6 | 0.1 | 1.8 | 3.6 | 1.0 | 17.5 | 5.8 | 73.7 | 27.3 | 132 | 27.1 | 300 | 54.3 | 909 | 2.3 | 20.5 | 10441 | 250 | 455 | 655 | 18.2 | 637 | 0.3 | 31.1 | 1.5 | 1.1 |
| WTC-10-03 | 0.2 | 13.6 | 0.4 | 4.5 | 6.3 | 1.7 | 27.2 | 7.9 | 91.6 | 31.5 | 150 | 30.1 | 325 | 59.3 | 1060 | 2.4 | 28.6 | 10457 | 360 | 600 | 749 | 26.8 | 722 | 0.3 | 9.0 | 1.8 | 0.8 |
| WTC-10-05 | 0.1 | 12.4 | 0.2 | 3.0 | 4.8 | 1.4 | 21.2 | 6.4 | 76.7 | 27.3 | 134 | 27.2 | 301 | 55.8 | 926 | 2.0 | 20.6 | 9468 | 267 | 430 | 671 | 21.8 | 649 | 0.4 | 16.7 | 1.4 | 1.0 |
| WTC-10-06 | 0.3 | 7.4 | 0.1 | 1.4 | 2.4 | 0.6 | 13.9 | 5.0 | 64.1 | 25.6 | 122 | 26.9 | 275 | 54.1 | 819 | 1.5 | 18.2 | 9806 | 78 | 113 | 598 | 12.1 | 586 | 0.2 | 9.2 | 0.4 | 0.8 |
| WTC-10-07 | 0.1 | 6.4 | 0.2 | 3.1 | 5.1 | 0.8 | 27.7 | 9.0 | 114 | 41.1 | 196 | 39.0 | 413 | 70.6 | 1299 | 2.2 | 17.1 | 10277 | 214 | 381 | 927 | 15.7 | 911 | 0.2 | 9.4 | 0.9 | 1.3 |
| WTC-10-10 | 0.0 | 12.8 | 0.1 | 2.2 | 3.9 | 1.1 | 19.2 | 6.2 | 77.4 | 29 | 143 | 29.6 | 330 | 61.1 | 992 | 2.6 | 24.3 | 9327 | 285 | 545 | 716 | 20.3 | 696 | 0.3 | 24.8 | 1.6 | 1.1 |
| WTC-10-12 | 0.1 | 11.8 | 0.3 | 3.3 | 4.6 | 1.2 | 20.4 | 6.0 | 72.7 | 25.3 | 122 | 25.2 | 279 | 50.4 | 861 | 1.7 | 18.6 | 9486 | 233 | 401 | 622 | 21.2 | 601 | 0.3 | 12.9 | 1.4 | 0.9 |
| WTC-10-13 | 0.3 | 9.2 | 0.3 | 2.3 | 3.2 | 0.4 | 17.2 | 6.4 | 86.5 | 33.4 | 169 | 36.9 | 439 | 81.4 | 1066 | 3.2 | 84.8 | 12150 | 104 | 680 | 886 | 15.7 | 870 | 0.1 | 8.0 | 1.5 | 0.4 |
| WTC-10-16 | 0.1 | 13.9 | 0.2 | 2.1 | 3.4 | 1.1 | 17.6 | 5.7 | 71.3 | 26.4 | 130 | 26.8 | 300 | 53.1 | 895 | 2.2 | 19.4 | 9102 | 240 | 403 | 652 | 21.0 | 631 | 0.4 | 17.8 | 1.3 | 1.1 |
| WTC-10-17 | 0.7 | 10.3 | 1.0 | 8.6 | 8.7 | 1.8 | 30.0 | 9.8 | 120 | 41.4 | 194 | 38.1 | 394 | 69.1 | 1320 | 2.5 | 18.8 | 11334 | 271 | 432 | 928 | 31.1 | 897 | 0.3 | 2.6 | 1.1 | 1.3 |
| WTC-10-20 | 0.4 | 10.8 | 0.8 | 6.8 | 8.6 | 1.7 | 31.5 | 10.5 | 126 | 44.3 | 207 | 42.0 | 433 | 73.7 | 1412 | 3.1 | 31.7 | 11258 | 367 | 747 | 997 | 29.1 | 968 | 0.3 | 3.5 | 1.7 | 1.0 |